Constructing Hyperbolic Polyhedra Using Newton's Method

Roland K. W. Roeder

CONTENTS

We demonstrate how to construct three-dimensional compact hyperbolic polyhedra using Newton's method. Under the restriction that the dihedral angles must be nonobtuse, Andreev's theorem [Andreev 70a, Andreev 70b] provides as necessary and sufficient conditions five classes of linear inequalities for the dihedral angles of a compact hyperbolic polyhedron realizing a given combinatorial structure C. Andreev's theorem also shows that the resulting polyhedron is unique, up to hyperbolic isometry. Our construction uses Newton's method and a homotopy to explicitly follow the existence proof presented by Andreev, providing both a very clear illustration of a proof of Andreev's theorem and a convenient way to construct three-dimensional compact hyperbolic polyhedra having nonobtuse dihedral angles.

As an application, we construct compact hyperbolic polyhedra having dihedral angles that are (proper) integer submultiples of π, so that the group Γ generated by reflections in the faces is a discrete group of isometries of hyperbolic space. The quotient $\mathbb{H}^3/\Gamma$ is hence a compact hyperbolic 3-orbifold, of which we study the hyperbolic volume and spectrum of closed geodesic lengths using SnapPea. One consequence is a volume estimate for a "hyperelliptic" manifold considered in [Mednykh and Vesnin 03].

1. INTRODUCTION

Andreev's theorem [Andreev 70a, Andreev 70b] provides a complete characterization of compact hyperbolic polyhedra having nonobtuse dihedral angles. See also [Roeder et al. 07, Roeder 04] for an alternative exposition on the classical proof. Other approaches to Andreev's theorem can be found in [Rivin and Hodgson 93, Hodgson 92, Thurston 80, Marden and Rodin 90, Bowers and Stephenson 96]. In this paper we show that the classical proof from [Andreev 70a, Andreev 70b, Roeder et al. 07, Roeder 04] is constructive when combined with Newton's method for solving nonlinear equations.

Combinatorial descriptions of hyperbolic polyhedra that are relevant to Andreev's theorem fall into three

2000 AMS Subject Classification: Primary: 52B10, 65H20, 52A55; Secondary 51M09, 65-04, 65-05

Keywords: Hyperbolic polyhedra, Andreev's theorem, Newton's method, polyhedral orbifolds

1058-6458/2007 $ 0.50 per page

classes: *simple, truncated*, and *compound*, all defined later in this section. The proof in [Roeder et al. 07, Roeder 04] provides an explicit continuous path in the space of polyhedra deforming a given simple polyhedron P to one of two that are easily constructed by hand: the N-faced prism Pr_N and the N-faced split prism D_N. We use Newton's method to follow such a path backward, deforming a computer realization of Pr_N or D_N to a computer realization of the desired polyhedron P. This technique, which has been well studied in the literature, is known as the homotopy method [Allgower and Georg 90, Blum et al. 98, Shub and Smale 93a, Shub and Smale 93b, Shub and Smale 93c, Shub and Smale 96, Álvarez 06]. We illustrate the construction of simple polyhedra in Sections 2.5, 2.6, and 2.7.

A similar deformation, again using Newton's method, allows us to construct truncated polyhedra from simple polyhedra, as shown in Section 2.8. In Section 2.9 we show how to construct a compound polyhedron as a gluing of two appropriate truncated polyhedra.

In this way, our program graphically illustrates Andreev's proof of existence for explicit examples. In fact, writing this program and working through Andreev's proof for some specific examples led to the detection of an error in the proof of existence, which has been corrected in [Roeder et al. 07, Roeder 04].

A further benefit of this program is the construction of polyhedra whose dihedral angles are proper integer submultiples of π. As a consequence of Poincaré's polyhedron theorem [Poincaré 83], the group Γ generated by reflections in the faces of such a polyhedron is a discrete group of isometries of hyperbolic space. The quotient $\mathbb{H}^3/\Gamma$ is hence a compact hyperbolic 3-orbifold, of which we study the hyperbolic volume and spectrum of closed geodesic lengths using SnapPea.[1] Such orbifolds and their covering manifolds have been studied extensively [Löbell 31, Vesnin 87, Mednykh and Vesnin 03, Vesnin 98, Garrison and Scott 03, Kellerhals 89, Reni 97]. In fact, the first example of a closed hyperbolic 3-manifold was obtained in this way in 1931 by Löbell [Löbell 31]. One consequence of our study is a volume estimate for a "hyperelliptic" manifold considered in [Mednykh and Vesnin 03]. (In fact, after this paper was written, a study of the volumes of right-angled hyperbolic polyhedra was undertaken by Taiyo Inoue in his doctoral thesis [Inoue 07]).

The reader should note that there are already excellent computer programs for experimentation with hyperbolic 3-manifolds. The program SnapPea constructs hyperbolic structures on knot and link complements, as well as the hyperbolic Dehn surgeries on these complements. SnapPea provides for the computation of a variety of geometry invariants of the computed hyperbolic structure. (See also [Adams et al. 91].) The program Snap provides a way of computing arithmetic invariants of hyperbolic manifolds. Both of these programs are quite easy to use and have allowed for vast levels of experimentation, including a nice census of low-volume hyperbolic manifolds and orbifolds.

An impressive generalization of SnapPea, called Orb, was recently developed by Damian Heard.[2] This program allows for the construction of hyperbolic orbifolds whose underlying topological space is $\mathbb{S}^3$ and whose singular set consists of an embedded graph. Many details about the theory of this program are available in Heard's doctoral thesis [Heard 05].

The experimentation done in this paper with the hyperbolic orbifolds obtained from polyhedral reflection groups is very modest in comparison. However, it is an alternative way to construct hyperbolic structures on certain orbifolds (and, in the future, possibly on manifold covers of these orbifolds) in a way that these structures can nicely be studied by SnapPea (as well as in the future with Snap, Orb, and other software).

Let $E^{3,1}$ be $\mathbb{R}^4$ with the indefinite metric $\|\mathbf{x}\|^2 = -x_0^2+x_1^2+x_2^2+x_3^2$. In this paper, we work in the hyperbolic space $\mathbb{H}^3$ given by the component of the subset of $E^{3,1}$ given by

$$\|\mathbf{x}\|^2 = -x_0^2 + x_1^2 + x_2^2 + x_3^2 = -1,$$

with $x_0 > 0$ and with the Riemannian metric induced by the indefinite metric

$$-dx_0^2 + dx_1^2 + dx_2^2 + dx_3^2.$$

The hyperplane orthogonal to a vector $\mathbf{v} \in E^{3,1}$ intersects $\mathbb{H}^3$ if and only if $\langle \mathbf{v}, \mathbf{v} \rangle > 0$. Let $\mathbf{v} \in E^{3,1}$ be a vector with $\langle \mathbf{v}, \mathbf{v} \rangle > 0$, and define

$$P_{\mathbf{v}} = \{\mathbf{w} \in \mathbb{H}^3 | \langle \mathbf{w}, \mathbf{v} \rangle = 0\}$$

and

$$H_{\mathbf{v}} = \{\mathbf{w} \in \mathbb{H}^3 | \langle \mathbf{w}, \mathbf{v} \rangle \leq 0\}$$

to be the hyperbolic plane orthogonal to $\mathbf{v}$ and the corresponding closed half-space.

[1] See http://www.ms.unimelb.edu.au/~snap.

[2] See http://www.ms.unimelb.edu.au/~snap/orb.html.

If one normalizes $\langle \mathbf{v}, \mathbf{v} \rangle = 1$ and $\langle \mathbf{w}, \mathbf{w} \rangle = 1$, the planes $P_{\mathbf{v}}$ and $P_{\mathbf{w}}$ in $\mathbb{H}^3$ intersect in a line if and only if $\langle \mathbf{v}, \mathbf{w} \rangle^2 < 1$, in which case their dihedral angle is $\arccos(-\langle \mathbf{v}, \mathbf{w} \rangle)$. They intersect in a single point at infinity if and only if $\langle \mathbf{v}, \mathbf{w} \rangle^2 = 1$; in this case their dihedral angle is 0.

A *hyperbolic polyhedron* is an intersection

$$P = \bigcap_{i=0}^{n} H_{\mathbf{v_i}}$$

having nonempty interior.

We will often use the Poincaré ball model of hyperbolic space, given by the unit ball in $\mathbb{R}^3$ with the metric

$$4\frac{dx_1^2 + dx_2^2 + dx_3^2}{(1 - \|\mathbf{x}\|^2)^2}$$

and the upper-half-space model of hyperbolic space, given by the subset of $\mathbb{R}^3$ with $x_3 > 0$ equipped with the metric

$$\frac{dx_1^2 + dx_2^2 + dx_3^2}{x_3^2}.$$

Both of these models are isomorphic to $\mathbb{H}^3$.

Hyperbolic planes in these models correspond to Euclidean hemispheres and Euclidean planes that intersect the boundary perpendicularly. Furthermore, these models are conformally correct; that is, the hyperbolic angle between a pair of such intersecting hyperbolic planes is exactly the Euclidean angle between the corresponding spheres or planes.

1.1 Combinatorial Polyhedra and Andreev's Theorem

A compact hyperbolic polyhedron P is topologically a three-dimensional ball, and its boundary is a 2-sphere $\mathbb{S}^2$. The face structure of P gives $\mathbb{S}^2$ the structure of a cell complex C whose faces correspond to the faces of P.

Considering only hyperbolic polyhedra with nonobtuse dihedral angles simplifies the combinatorics of any such C:

Proposition 1.1.

(a) *A vertex of a nonobtuse hyperbolic polyhedron P is the intersection of exactly three faces.*

(b) *For such a P, we can compute the angles of the faces in terms of the dihedral angles; these angles are also at most $\pi/2$.*

This proposition is well-known; see, for example [Roeder et al. 07, Roeder 04].

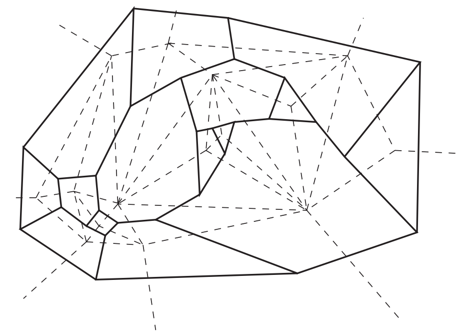

FIGURE 1. An abstract polyhedron C and the dual complex C^* (dashed).

The fundamental axioms of incidence place the following, obvious, further restrictions on the complex C:

- Every edge of C belongs to exactly two faces.
- A nonempty intersection of two faces is either an edge or a vertex.
- Every face contains not fewer than three edges.

Any trivalent cell complex C on $\mathbb{S}^2$ that satisfies the three conditions above is an *abstract polyhedron*. Since C must be a trivalent cell complex on $\mathbb{S}^2$, its dual, C^*, has only triangular faces, and the three conditions above ensure that it is a simplicial complex on $\mathbb{S}^2$. Figure 1 shows an abstract polyhedron C drawn in the plane (i.e., with one of the faces corresponding to the region outside of the figure). The dual complex is also shown, in dashed lines.

We call a simple closed curve Γ formed of k edges of C^* a *k-circuit*, and if all of the endpoints of the edges of C intersected by Γ are distinct, we call such a circuit a *prismatic k-circuit*. Figure 2 shows the same abstract polyhedron as Figure 1, except that this time, the prismatic 3-circuits are dashed, the prismatic 4-circuits are dotted, and the dual complex is not shown.

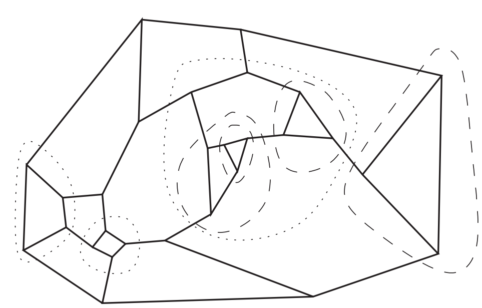

FIGURE 2. Abstract polyhedron C with prismatic 3-circuits (dashed) and prismatic 4-circuits (dotted).

We say that a combinatorial polyhedron C is *simple* if it has no prismatic 3-circuits, *truncated* if C has prismatic 3-circuits and each surrounds a single triangular face on one side, and otherwise, we call C *compound.* The combinatorial polyhedron shown in Figures 1 and 2 is compound.

Theorem 1.2. (Andreev's theorem) *Let C be an abstract polyhedron with more than four faces and suppose that nonobtuse angles $\mathbf{a}_i$ are given corresponding to edge e_i of C. There is a compact hyperbolic polyhedron P whose faces realize C with dihedral angle $\mathbf{a}_i$ at each edge e_i if and only if the following five conditions all hold:*

(1) *For each edge e_i, $\mathbf{a}_i > 0$.*

(2) *Whenever three distinct edges e_i, e_j, e_k meet at a vertex, $\mathbf{a}_i + \mathbf{a}_j + \mathbf{a}_k > \pi$.*

(3) *Whenever Γ is a prismatic 3-circuit intersecting edges e_i, e_j, e_k, then $\mathbf{a}_i + \mathbf{a}_j + \mathbf{a}_k < \pi$.*

(4) *Whenever Γ is a prismatic 4-circuit intersecting edges e_i, e_j, e_k, e_l, then $\mathbf{a}_i + \mathbf{a}_j + \mathbf{a}_k + \mathbf{a}_l < 2\pi$.*

(5) *Whenever there is a four-sided face bounded by edges e_1, e_2, e_3, and e_4, enumerated successively, with edges $e_{12}, e_{23}, e_{34}, e_{41}$ entering the four vertices (edge e_{ij} connecting to the ends of e_i and e_j), then*

$$\mathbf{a}_1 + \mathbf{a}_3 + \mathbf{a}_{12} + \mathbf{a}_{23} + \mathbf{a}_{34} + \mathbf{a}_{41} < 3\pi$$

and

$$\mathbf{a}_2 + \mathbf{a}_4 + \mathbf{a}_{12} + \mathbf{a}_{23} + \mathbf{a}_{34} + \mathbf{a}_{41} < 3\pi.$$

Furthermore, this polyhedron is unique up to isometries of $\mathbb{H}^3$.

Corollary 1.3. *If C is simple, i.e., has no prismatic 3-circuits, there exists a unique hyperbolic polyhedron realizing C with dihedral angles $2\pi/5$.*

For a given C, let E be the number of edges of C. The subset of $(0, \pi/2]^E$ satisfying these linear inequalities will be called the *Andreev polytope* A_C. Since A_C is determined by linear inequalities, it is convex.

Andreev's restriction to nonobtuse dihedral angles is emphatically necessary to ensure that A_C is convex. Without this restriction, the corresponding space Δ_C of dihedral angles of compact (or finite-volume) hyperbolic polyhedra realizing a given C is not convex [Díaz 97]. In fact, recent work by Díaz [Díaz 06] provides a detailed analysis of this space Δ_C of dihedral angles for the class of abstract polyhedra C obtained from the tetrahedron by successively truncating vertices. Her work nicely illustrates the types of nonlinear conditions that are necessary in a complete analysis of the larger space of dihedral angles Δ_C.

The work of Rivin [Rivin 96, Rivin 93] shows that the space of dihedral angles for ideal polyhedra forms a convex polytope, *without the restriction to nonobtuse angles.* See also [Guéritaud 04].

Notice also that the hypothesis that the number of faces is greater than four is also necessary, because the space of nonobtuse dihedral angles for compact tetrahedra is not convex [Roeder 06]. Conditions (1)–(5) remain necessary for compact tetrahedra, but they are no longer sufficient.

In [Bao and Bonahon 02] a similar classification theorem for hyperideal polyhedra is proved. Finally, the papers of Vinberg on discrete groups of reflections in hyperbolic space [Alekseevskij et al. 93, Vinberg 67, Vinberg 85, Vinberg 91, Vinberg and Shvartsman 93] are also closely related, as well as the work in [Chow and Luo 03] and [Schlenker 00, Schlenker 98, Schlenker 06].

Much attention has been focused on Andreev's theorem from the viewpoint of circle packings and circle patterns. Given a polyhedron P in the upper-half-space model of $\mathbb{H}^3$, the planes supporting the faces of P intersect the boundary at infinity $x_3 = 0$ in a pattern of circles (and straight lines), each with an orientation specifying "on which side" the polyhedron P is located. Similarly, from such a pattern of circles and orientations one can reconstruct a polyhedron P.

The works [Thurston 80], [Marden and Rodin 90], and [Bowers and Stephenson 96] all follow this approach to Andreev's theorem. In fact, there is a beautiful computer program known as Circlepack,[3] written by Ken Stephenson, that computes circle packings and patterns of circles with specified angles of overlap. All of the proofs from this point of view use the conformal structure of the Riemann sphere $\hat{\mathbb{C}} = \partial_\infty \mathbb{H}^3$ and use the correspondence between conformal automorphisms of $\hat{\mathbb{C}}$ with isometries of $\mathbb{H}^3$.

Instead of using the conformal structure on $\partial_\infty \mathbb{H}^3$, in this paper we will work specifically with the metric structure of $\mathbb{H}^3$. (However, there is certainly some significant overlap with the results in [Thurston 80, Marden and Rodin 90, Bowers and Stephenson 96] and with the capabilities of the computer program CirclePack.)

[3]See http://www.math.utk.edu/~kens/CirclePack/.

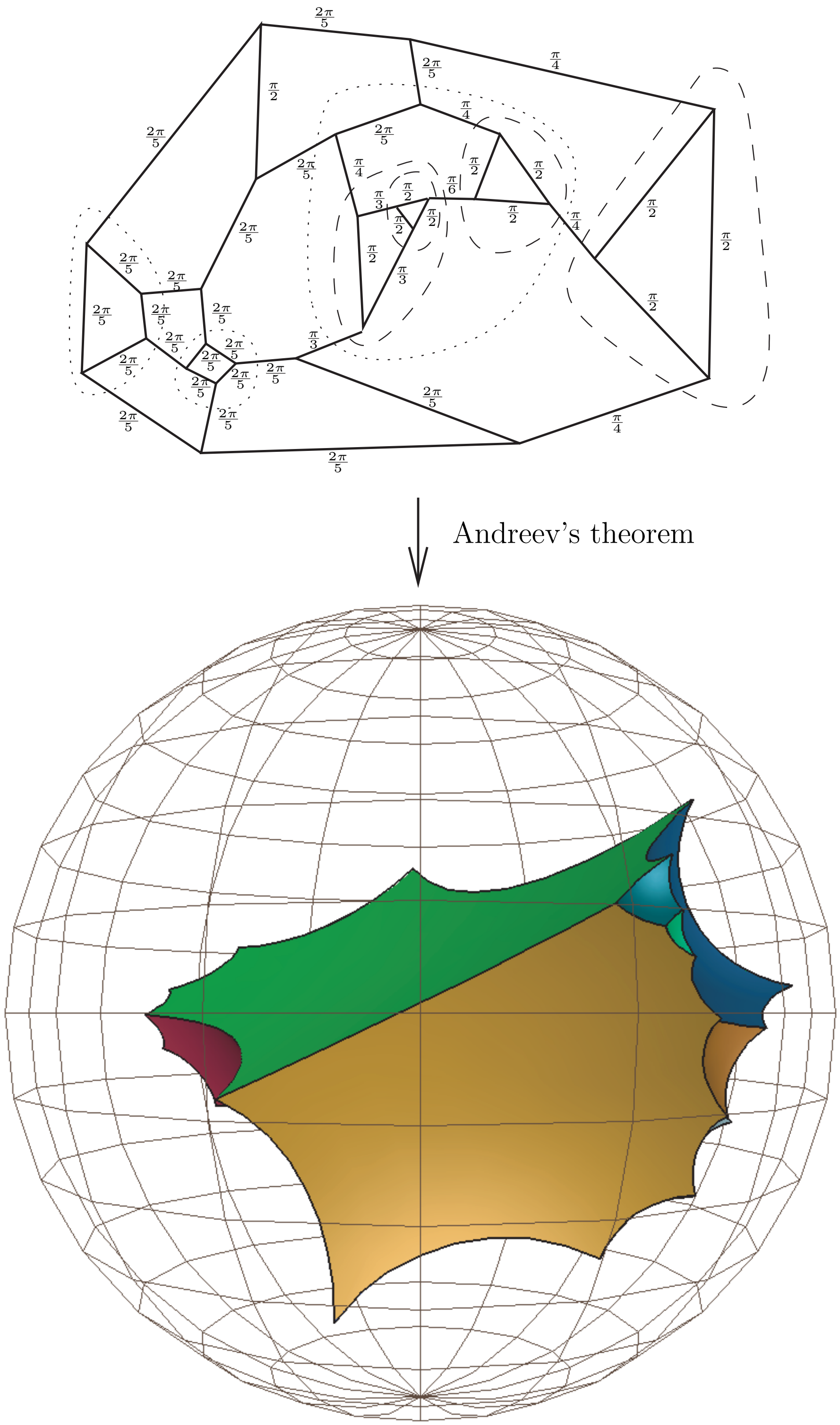

FIGURE 3. Illustration of Andreev's theorem.

We will now explain the implementation of a computer program whose input is the combinatorial polyhedron C and a dihedral-angle vector $\mathbf{a} \in A_C$ and whose output is a hyperbolic polyhedron realizing the pair $(C, \mathbf{a})$.

1.2 An Example

Figure 3 shows an explicit example of the data $(C, \mathbf{a})$ and the resulting polyhedron displayed in the conformal ball model using the computer program Geomview.[4]

1.3 Outline of the Proof of Andreev's Theorem

In this section, we recall the major steps from the proof of Andreev's theorem that were presented in [Roeder et al. 07, Roeder 04].

Let C be a trivalent abstract polyhedron with N faces. We say that a hyperbolic polyhedron $P \subset \mathbb{H}^3$ *realizes* C if there is a cellular homeomorphism from C to ∂P (i.e., a homeomorphism mapping faces of C to faces of P, edges of C to edges of P, and vertices of C to vertices of P). We will call each isotopy class of cellular homeomorphisms $\phi : C \to \partial P$ a *marking* on P.

We defined $\mathcal{P}_C$ to be the set of pairs (P, ϕ) such that ϕ is a marking with the equivalence relation specifying that $(P, \phi) \sim (P', \phi')$ if there exists an automorphism $\rho : \mathbb{H}^3 \to \mathbb{H}^3$ such that $\rho(P) = P'$, and both ϕ' and $\rho \circ \phi$ represent the same marking on P'.

Proposition 1.4. *The space $\mathcal{P}_C$ is a manifold of dimension $3N - 6$ (perhaps empty).*

The proof is relatively standard and can be found in [Roeder et al. 07, Roeder 04].

Since the edge graph of C is trivalent, the number E of edges of C is the same as the dimension of $\mathcal{P}_C$. Given any $P \in \mathcal{P}_C$, let $\alpha(P) = (\mathbf{a}_1, \mathbf{a}_2, \mathbf{a}_3, \dots)$ be the E-tuple consisting of the dihedral angles of P at each edge (according to some fixed numbering of the edges of C). This map α is obviously continuous with respect to the topology on $\mathcal{P}_C$, which it inherits from its manifold structure.

We let $\mathcal{P}_C^0$ be the subset of $\mathcal{P}_C$ consisting of polyhedra with nonobtuse dihedral angles. To establish Andreev's theorem, we proved the following statement:

Theorem 1.5. *For every abstract polyhedron C having more than four faces, the mapping $\alpha : \mathcal{P}_C^0 \to A_C$ is a homeomorphism.*

There were two major steps in the proof:

Proposition 1.6. *If $\mathcal{P}_C^0 \neq \varnothing$, then $\alpha : \mathcal{P}_C^0 \to A_C$ is a homeomorphism.*

We checked that $\alpha(\mathcal{P}_C^0) \subset A_C$ by showing that conditions (1)–(5) are necessary. There is an open subset $\mathcal{P}_C^1 \subset \mathcal{P}_C$ containing $\mathcal{P}_C^0$ on which one can prove that $\alpha : \mathcal{P}_C^1 \to \mathbb{R}^E$ is injective, using a modification of Cauchy's rigidity theorem for Euclidean polyhedra. This gives the uniqueness part of Andreev's theorem. Using invariance of domain, it also gives that $\alpha : \mathcal{P}_C^1 \to \mathbb{R}^E$ is a local homeomorphism. Because $\mathcal{P}_C^0 \subset \mathcal{P}_C^1$, α restricted to $\mathcal{P}_C^0$ is a local homeomorphism as well.

We then showed that $\alpha : \mathcal{P}_C^0 \to A_C$ is proper, which amounts to showing that if a sequence of polyhedra P_i in $\mathcal{P}_C^0$ is degenerate (i.e., leaves $\mathcal{P}_C^0$), then the sequence $\alpha(P_i)$ tends to ∂A_C. The fact that $\alpha : \mathcal{P}_C^0 \to A_C$ is a proper local homeomorphism was sufficient to show that $\alpha(\mathcal{P}_C^0)$ is open and closed in A_C.

Proposition 1.7. *If $A_C \neq \varnothing$, then $\mathcal{P}_C^0 \neq \varnothing$.*

The second step was much more difficult because for each C with nonempty A_C one needed to construct some polyhedron realizing C (with nonobtuse dihedral angles). In fact, the proof of Proposition 1.7 outlines a scheme for how to construct a polyhedron realizing C. Section 2 of this paper outlines how to follow this scheme explicitly on the computer using Newton's method and a homotopy method.

2. A METHOD FOR CONSTRUCTING ANDREEV POLYHEDRA

2.1 Representing Polyhedra on the Computer

All the constructions of polyhedra in this paper are done using Matlab[5] or the Free Software Foundation alternative Octave,[6] and all of the polyhedra are displayed in Geomview. When doing calculations, we represent a hyperbolic polyhedron P having N faces by specifying N outward-pointing normal vectors $\mathbf{v}_1, \dots, \mathbf{v}_N$ each with $\langle \mathbf{v}_i, \mathbf{v}_i \rangle = 1$, so that $P = \bigcap_{i=1}^n H_{\mathbf{v}_i}$.

Although such a list of N vectors is sufficient to specify P, in order to avoid repeated computation of the combinatorial structure of P from these vectors we additionally specify the adjacency matrix and a list of all plane triples meeting at a vertex. These three items are described

[4]See www.geomview.org.

[5]See www.mathworks.com.

[6]See www.octave.org.

in a Matlab struct `P`, with `P.faces`, `P.adjacency`, and `P.vert` holding the data mentioned above, respectively.

For example, the data for the polyhedron shown in Section 1.2 are stored in Matlab as follows:

```
New_poly =
         vert: [28x3 double]
        faces: [16x4 double]
    adjacency: [16x16 double]

New_poly.faces =
   36.5078  -10.7624   -0.3090  -34.8983
    4.9237   -1.5291   -1.2342   -4.6240
   -0.0000    0.8660   -0.5000   -0.0000
    4.5134   -2.1988   -2.3943   -3.2868
    2.7290   -1.9854   -0.3091   -2.1000
   13.3691   -5.0338   -0.3090  -12.4216
   65.0863  -19.6363   -2.7939  -61.9987
   35.9576   -9.6209   -1.5515  -34.6262
   51.5713  -13.3145   -0.3090  -49.8320
    5.8378   -0.5352   -0.3090   -5.8905
   -0.0000    0.0000    1.0000    0.0000
    1.2179   -1.4082   -0.7071    0.0000
   -7.8692    2.1329    3.6943    6.6879
    3.4039   -1.5744   -2.7269   -1.6344
   -1.0781    0.5773   -0.0000   -1.3524
   -2.1544    0.9964    1.7260   -1.2921

New_poly.adjacency =
  1   0   0   0   0   1   1   1   1   0   1   0   0   0   0   0
  0   1   1   1   1   1   1   1   0   1   0   0   1   0   0   0
  0   1   1   1   0   0   0   0   0   1   1   1   1   1   1   1
  0   1   1   1   1   0   0   0   0   0   0   1   1   1   0   0
  0   1   0   1   1   1   0   0   0   0   1   1   0   0   0   0
  1   1   0   0   1   1   1   0   0   0   1   0   0   0   0   0
  1   1   0   0   0   1   1   1   0   0   0   0   0   0   0   0
  1   1   0   0   0   0   1   1   1   1   0   0   0   0   0   0
  1   0   0   0   0   0   0   1   1   1   1   0   0   0   0   0
  0   1   1   0   0   0   0   1   1   1   1   0   0   0   0   0
  1   0   1   0   1   1   0   0   1   1   1   1   0   0   1   0
  0   0   1   1   1   0   0   0   0   0   1   1   0   1   1   1
  0   1   1   1   0   0   0   0   0   0   0   0   1   0   0   0
  0   0   1   1   0   0   0   0   0   0   0   1   0   1   0   0
  0   0   1   0   0   0   0   0   0   0   1   1   0   0   1   1
  0   0   1   0   0   0   0   0   0   0   0   1   0   0   1   1

New_poly.vert =
     3     4    14
     6     5    11
     4    12     5
    12     5    11
     1     6     7
     1     7     8
     1     8     9
     1     9    11
    10     9    11
     1     6    11
     2     3    13
     2     4     5
     2     5     6
     2     6     7
     2     7     8
     9     8    10
     2     8    10
     2    10     3
    11    10     3
     2     4    13
     3     4    13
     3    12    14
     4    12    14
    11     3    15
    11    12    15
     3    12    16
     3    15    16
    12    15    16
```

We display the polyhedra in Geomview using the hyperbolic mode and specifying the conformal ball model. The file format most convenient for our use is the Object File Format `New_poly.off`. The first line of an Object format file specifies the number of vertices, the number of faces, and the number of edges of P in that order: `num_vert num_faces num_edges`.

The next block of data is a list of the coordinates of vertices as points in the unit ball. (In fact, these are the coordinates of points in the projective model for $\mathbb{H}^3$, not the Poincaré ball model that we described in the introduction.) The last block of data is a list of the faces, with each face given by $\texttt{vertex}_1$ $\texttt{vertex}_2$ $\texttt{...vertex}_n$ `colorspec`, where the faces are spanned by vertex_1 $\texttt{vertex}_2\texttt{...vertex}_n$, and `colorspec` is an integer telling Geomview what color to assign to the face:

```
28 16 42

0.093414 0.626297 -0.759378
0.668701 -0.423986 0.508660
0.480895 0.480927 -0.729094
0.533074 -0.046431 -0.835831
0.000602 -0.321164 0.944739
-0.109909 -0.298793 0.946284
-0.257482 -0.413626 0.871178
-0.241511 -0.517345 0.817366
-0.394737 -0.502851 0.762029
0.039860 -0.522084 0.841280
-0.198257 0.894806 -0.304826
0.473945 0.834475 -0.252208
0.632626 0.016126 0.705772
0.030462 -0.199457 0.975695
-0.112537 -0.193119 0.972142
-0.373893 -0.377061 0.844031
-0.376723 -0.130280 0.905450
-0.802208 0.544817 0.123196
-0.869841 -0.223571 -0.241933
0.160888 0.910483 -0.333052
0.007468 0.802257 -0.570580
0.104069 0.367146 -0.917226
0.301741 0.507113 -0.798909
-0.023848 -0.005394 -0.995609
0.158629 -0.006953 -0.985479
0.065661 0.192695 -0.976218
0.028183 0.094604 -0.992919
0.091162 0.094314 -0.989423

5 5 6 7 9 4 1
8 17 16 14 13 12 11 19 10 2
9 20 10 17 18 23 26 25 21 0 3
6 20 19 11 2 22 0 4
5 3 2 11 12 1 5
5 9 4 13 12 1 6
4 5 14 13 4 7
5 6 15 16 14 5 8
4 7 8 15 6 9
5 15 16 17 18 8 10
8 3 24 23 18 8 7 9 1 11
7 3 24 27 25 21 22 2 12
3 19 20 10 13
3 21 22 0 14
4 24 27 26 23 15
3 26 27 25 16
```

Something is lacking when one views the polyhedra displayed in the two-dimensional images shown in this paper. To alleviate this difficulty, the Matlab and OFF files associated with each polyhedron that is constructed in this paper are included as supplementary materials online at http://www.expmath.org/expmath/volumes/16/16.4/Roeder/supplement.zip See the Geomview website[7] for full details on the use of Geomview.

2.2 The Desired Polyhedron as a Solution to $4N$ Quadratic Equations in $4N$ Unknowns

The proof of Andreev's theorem gives that $\alpha_C : \mathcal{P}_C^0 \to A_C$ is a homeomorphism, so the problem of constructing a polyhedron P realizing $(C, \mathbf{a})$ can be expressed as the problem of finding a solution P to the equation $\alpha_C(P) = \mathbf{a}$.

Instead of working in $\mathcal{P}_C^0$, we write the desired polyhedron as a solution of a system of $4N$ quadratic equations in $4N$ variables, where N is the number of faces of C. Our solution is N vectors $\mathbf{v_1}, \dots, \mathbf{v_N} \in E^{3,1}$ satisfying

- $\langle \mathbf{v_i}, \mathbf{v_i} \rangle = 1$,
- $\langle \mathbf{v_j}, \mathbf{v_j} \rangle = -\cos(\mathbf{a}_{i,j})$ if faces i and j are adjacent in C and their common edge is assigned dihedral angle $\mathbf{a}_{i,j}$.

These equations impose $E + N$ conditions on $4N$ variables, where C has N faces and E edges.

As mentioned in Section 1.3, we have $E = 3N - 6$, so we have imposed $4N - 6$ conditions on $4N$ variables. We impose six additional conditions in order to have the same number of equations and unknowns. We normalize by requiring that a chosen vector $\mathbf{v_i}$ perpendicular to one of the faces agree with some given $\mathbf{v}$ (where $\mathbf{v}$ is chosen such that $\langle \mathbf{v}, \mathbf{v} \rangle = 1$). We then require that one of the vertices on the face perpendicular to $\mathbf{v_i}$ be at a given point $\mathbf{w}$ in the plane $P_\mathbf{v}$ and that a vertex adjacent to this vertex be on a given line l in $P_\mathbf{v}$ through $\mathbf{w}$. One can check that these normalizations provide 3, 2, and 1 additional equations respectively. (Notice that each of the six equations for this normalization is linear.) We denote the normalization by the triple $(\mathbf{v}, \mathbf{w}, l)$.

We denote the resulting quadratic map by $F_{C,(\mathbf{v},\mathbf{w},l)} : \mathbb{R}^{4N} \to \mathbb{R}^{4N}$. Typically we will mention the normalization only when necessary. We denote the conditions described above for the right-hand side of the equations $F(x) = y$ by $(\mathbf{a}, 0)$, where the $\mathbf{a}$ from this pair is shorthand for the conditions $\langle \mathbf{v_i}, \mathbf{v_i} \rangle = 1$ and $\langle \mathbf{v_j}, \mathbf{v_j} \rangle = -\cos(\alpha_{i,j})$ if faces i and j are adjacent in C, and the 0 represents the fact that the normalization $(\mathbf{v}, \mathbf{w}, l)$ is satisfied.

[7] www.geomview.org.

Andreev's theorem asserts that if $\mathbf{a} \in A_C$, there is a real solution to $F_{C,(\mathbf{v},\mathbf{w},l)}(x) = (\mathbf{a}, 0)$ corresponding to N vectors $\mathbf{v}_1, \dots, \mathbf{v}_N$ in $E^{3,1}$ such that $P = \bigcap_{i=0}^n H_{\mathbf{v_i}}$ realizes the pair $(C, \mathbf{a})$.

There are many sensible ways to numerically solve a system of quadratic equations in the same number of equations as unknowns. These include the prepackaged nonlinear solvers in Matlab, Maple, and Mathematica; Newton's method; and Gröbner-basis techniques, as well as fancier quadratically constrained solvers.

The difficulty is that with $4N$ quadratic equations in $4N$ unknowns, Bézout's theorem states that there will typically be $16N^2$ solutions. On their own, these solvers cannot easily be adapted to find the specific solution corresponding to a convex polyhedron without first finding all solutions (or at least all real solutions) and then examining each solution to check whether it corresponds to the desired polyhedron. Since some solutions may be much harder to find than others, one could spend significant computation time pursuing solutions that are not of interest.

One way to ensure that the solution does correspond to a compact convex polyhedron is to use an iterative method, such as Newton's method, for which an initial condition that is sufficiently close to a given solution is guaranteed to converge to that root, in combination with a homotopy that guarantees that the nearest root is always the root that corresponds to a compact convex polyhedron. This is our approach, which we describe in greater detail in the next few sections. We are not entirely sure that this method is faster than finding all of the roots by "brute force" and then checking each solution to see whether it is the desired one, but our approach has the additional benefit that it explicitly follows Andreev's proof of existence, providing insight into how this proof works for specific examples.

2.3 Newton's Method and Homotopy Methods

Given two vector spaces V and W of the same dimension and a mapping $F : V \to W$, the associated Newton map $N_F : V \to V$ is given by the formula

$$N_F(\mathbf{x}) = \mathbf{x} - [DF(\mathbf{x})]^{-1}(F(\mathbf{x})). \qquad (2\text{–}1)$$

If the roots of F are nondegenerate, i.e., $DF(r_i)$ is invertible for each root r_i of F, then the roots of F correspond bijectively to superattracting fixed points of N_F.

Kantorovich's theorem [Kantorovič 49] gives a precise lower bound on the size of the basin of attraction for a root.

Theorem 2.1. (Kantorovich's theorem.) *Let $\mathbf{a_0}$ be a point in $\mathbb{R}^n$, U an open neighborhood of $\mathbf{a_0}$ in $\mathbb{R}^n$, and $F : U \to \mathbb{R}^n$ a differentiable mapping with $[DF(\mathbf{a_0})]$ invertible.*

Let U_0 be the open ball of radius $|[DF(\mathbf{a_0})]^{-1}F(\mathbf{a_0})|$ centered at $\mathbf{a_1} = N_F(\mathbf{a_1})$. If $U_0 \subset U$ and $[DF(\mathbf{x})]$ satisfy the Lipschitz condition $\| DF(\mathbf{u_1}) - DF(\mathbf{u_2}) \| \leq M|\mathbf{u_1} - \mathbf{u_2}|$ for all $\mathbf{u_1}, \mathbf{u_2} \in U_0$, and if the inequality

$$|F(\mathbf{a_0})| \cdot |[DF(\mathbf{a_0})]^{-1}|^2 M \leq \frac{1}{2} \qquad (2\text{–}2)$$

is satisfied, then the equation $F(\mathbf{x}) = 0$ has a unique solution in U_0, and Newton's method with initial guess $\mathbf{a_0}$ converges to it.

For a proof of Kantorovich's theorem, see [Hubbard and Hubbard 99] or the original source [Kantorovič 49].

While the dynamics near a fixed point can be easily understood by Kantorovich's theorem, the global dynamics of Newton's method can be very complicated, with loci of indeterminacy and critical curves where DN is not injective. In fact, the study of the dynamics of Newton's method to solve for the common roots of a pair of quadratic polynomials in $\mathbb{C}^2$ is a field of active research [Hubbard and Papadopol 07, Roeder 07]. We expect that the global dynamics of the Newton map to solve $F_{C,(\mathbf{v},\mathbf{w},l)}(x) = (\mathbf{a}, 0)$ are even significantly more complicated than those in [Hubbard and Papadopol 07, Roeder 07]. In particular, we have no reason to expect that a general initial condition in R^{4N} will converge under iteration of N_F to any solution of $F_{C,(\mathbf{v},\mathbf{w},l)}(x) = (\mathbf{a}, 0)$ nor to the specific solution representing a convex compact polyhedron P.

An approach that can sometimes be used to avoid the difficulties with the global dynamics of Newton's method is the homotopy method. Suppose that you want to solve $g(x) = y$. The idea is to replace this equation by a family that depends continuously on a single variable:

$$g_t(x_t) = y_t,$$

so that g_1 is the same function as g, and $y_1 = y$, while $g_0(x) = y_0$ is an equation for which you already know a solution x_0.

Choose k points $0 = t_1, t_2, \ldots, t_k = 1$. If k is sufficiently large, then x_{t_1} may be in the basin of attraction of Newton's method for $f_{t_2}(x) = y_{t_2}$. In this case, you can solve for x_{t_2} and can attempt to solve for x_{t_3} using Newton's method for $f_{t_3}(x) = y_{t_3}$ with initial condition x_{t_2}. Repeating this procedure, if possible, leads to the solution $x_1 = x_{t_k}$.

While this is obviously a very powerful method, there are many difficulties in choosing appropriate paths $g_t(x_t) = y_t$ and appropriate subdivisions $0 = t_1, t_2, \ldots, t_k = 1$. It is necessary to check that the conditions for Kantorovich's theorem are satisfied by x_{t_j} for the equation $f_{t_{j+1}}(x) = y_{t_{j+1}}$. The biggest difficulty is to avoid the situation in which the derivative $\frac{\partial}{\partial x} f_t$ is singular for some t. Such points are described as being in the *discriminant variety*, and choosing paths that avoid the discriminant variety is a big program of research. These difficulties are discussed extensively by many authors, including Shub and Smale, in [Blum et al. 98, Allgower and Georg 90, Shub and Smale 93a, Shub and Smale 93b, Shub and Smale 93c, Shub and Smale 96], and [Álvarez 06].

The proof of Andreev's theorem in [Roeder et al. 07, Roeder 04] provides an explicit path that we can use for a homotopy method to construct any simple polyhedron P as a continuous deformation of either the prism Pr_N or the split prism D_N, both of which can be easily constructed "by hand." We will use this path for our homotopy method: repeatedly using a polyhedron realizing a point on the path as initial condition and solving for a polyhedron slightly further on the path, chosen so that the dynamics of Newton's method converge to the correct solution of F.

With a similar path we can use the homotopy method again to construct any truncated polyhedron for which $A_C \neq \varnothing$. We take a continuous deformation of a simple polyhedron until the vertices to be truncated pass $\partial_\infty \mathbb{H}^3$, and then add a finite number of additional triangular faces intersecting the appropriate triples of faces perpendicularly. Compound polyhedra are then constructed as gluings of a finite number of truncated polyhedra.

Proposition 2.2. *The quadratic equation F has a uniform Lipschitz constant on R^{4N} depending only on the combinatorics of C.*

Proof: The proof is merely the observation that F is quadratic, so each of the second derivatives is constant. $\square$

While we have checked that F is Lipschitz, we make no effort to bound the norm of the derivative $[DF]$ away from zero (hence avoiding the discriminant variety). In fact, for a typical problem this is very hard to do. Instead, we merely try the homotopy method with the path mentioned in the preceding paragraph, and we show that the method works for all of the constructions that we at-

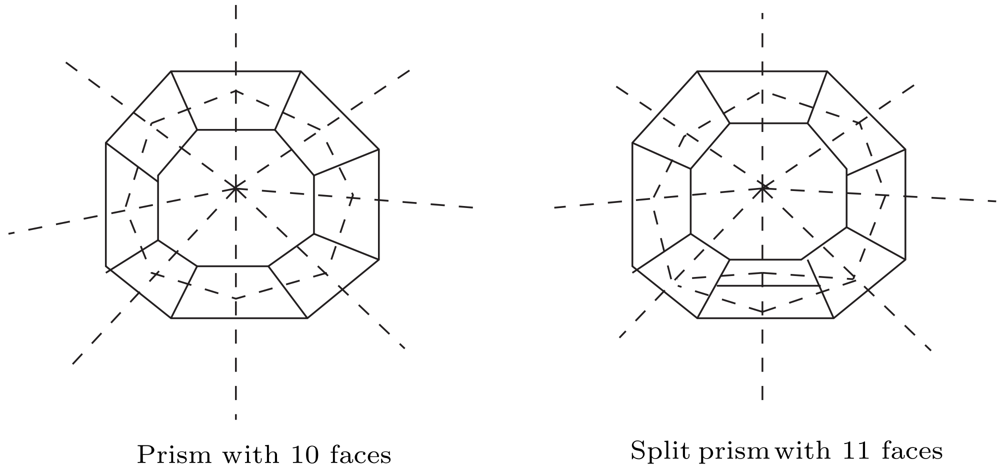

FIGURE 4. Combinatorial types for the prism Pr_N and the split prism D_N.

tempt. It may be interesting to provide a more rigorous basis for our use of Newton's method and the current choice of path.

2.4 Deforming a Given Polyhedron Using Newton's Method

Given a polyhedron P realizing C with dihedral angles $\mathbf{a} \in A_C$, it is easy to use Newton's method to deform P into a new polyhedron P' having any other angles $\mathbf{a}' \in A_C$ in the following way: since A_C is a convex polytope, choose the line segment between $\mathbf{a}$ and $\mathbf{a}'$ and subdivide this segment into K equally distributed points $\mathbf{a} = \mathbf{a}^0, \mathbf{a}^1, \mathbf{a}^2, \dots, \mathbf{a}^{K-1} = \mathbf{a}'$. Then we use Newton's method with initial condition corresponding to P to solve for a polyhedron P_1 with dihedral angles $\mathbf{a}^1$. We then repeat, using P_1 as initial condition for Newton's method to solve for a polyhedron P_2 with dihedral angles $\mathbf{a}^2$, and continue until we reach P' realizing $\mathbf{a}'$. If the homotopy method has worked, then each step of Newton's method converges; otherwise, we can try a larger number of subdivisions K, or attempt to check whether the path has hit the discriminant variety.

In all of the calculations within this paper, when deforming the angles of a given polyhedron P within A_C, we use K between 100 and 300 subdivisions, although this is sometimes significant overkill.

We consider it sufficient to show how to use Newton's method to construct some polyhedron P with nonobtuse dihedral angles for every C that has $A_C \neq \varnothing$. From this P one can construct any other $P' \in \mathcal{P}_C^0$ using the deformation described above. (The ease with which one can deform the angles of a given polyhedron is an additional benefit of our homotopy method.)

In the next sections we will see how to connect individual paths in $A_{C_1}, \dots, A_{C_k}$ so as to construct compact polyhedra realizing C_1 as a sequence of deformations of a compact polyhedron realizing C_k.

2.5 Simple Polyhedra and Whitehead Moves

Recall that if C is simple, then $\left(\frac{2\pi}{5}, \dots, \frac{2\pi}{5}\right) \in A_C$. The goal of this section and the following is to demonstrate the construction of a polyhedron P realizing any simple C with these dihedral angles.

Andreev's theorem provides a sequence of elementary changes (Whitehead moves) for reducing the combinatorics of C to one of the two combinatorial polyhedra D_N or Pr_N depicted in Figure 4.

In this section we show how to create polyhedra realizing D_N and Pr_N and how to do the Whitehead moves using Newton's method.

Lemma 2.3. *Let Pr_N and D_N be the abstract polyhedra corresponding to the N-faced prism and the N-faced "split prism," as illustrated in Figure 4. If $N > 4$, then $\mathcal{P}^0_{\mathrm{Pr}_N}$ is nonempty, and if $N > 7$, then $\mathcal{P}^0_{D_N}$ is nonempty.*

2.5.1 Construction. Construct a regular polygon with $N-2$ sides in the disk model for $\mathbb{H}^2$. (We have $N-2 \geq 3$, since $N \geq 5$.) We can do this with the angles arbitrarily small. Now view $\mathbb{H}^2$ as the equatorial plane of $\mathbb{H}^3$, and consider the hyperbolic planes perpendicular to the equatorial plane containing the sides of the polygon. In Euclidean geometry these are hemispheres with centers

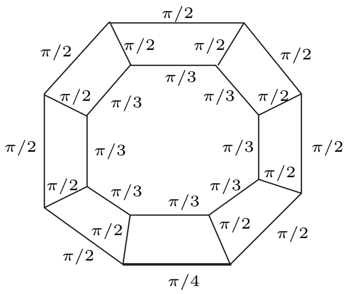

FIGURE 5. Specification of dihedral angles in the construction of D_N.

on the boundary of the equatorial disk. The dihedral angles of these planes are the angles of the polygon.

Consider two hyperbolic planes close to the equatorial plane, one slightly above and one slightly beneath, both perpendicular to the z-axis. These will intersect the previous planes at angles slightly smaller than $\pi/2$. The region defined by these N planes makes a hyperbolic polyhedron realizing the cell structure of the prism. Note that our construction completes the proof of Proposition 1.6 for the special case $C = \mathrm{Pr}_N$, $N \geq 5$.

For $N > 7$ we will construct D_N by cutting it into two prisms each with $N-1$ faces and the dihedral angles shown in Figure 5.

These angles satisfy Andreev's conditions (1)–(5), so we can use Newton's method to deform the prism constructed in the previous paragraph to have these angles. When we glue this prism to its mirror image, the edges labeled $\pi/2$ on the outside disappear as edges, and the edges labeled on the outside by $\pi/4$ glue together to become an edge with dihedral angle $\pi/2$. Hence, we have constructed a polyhedron realizing D_N, assuming $N > 7$. Notice that when $N \leq 7$, the combinatorics of D_N coincide with those of Pr_N.

Assume that the two vertices incident at an edge e are trivalent. A Whitehead move $Wh(e)$ on edge e is given by the local change of the abstract polyhedron described in Figure 6. The Whitehead move in the dual complex is dashed. Often we will find it convenient to describe the

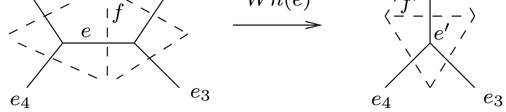

FIGURE 6. Whitehead move on edge e.

Whitehead move entirely in terms of the dual complex, in which case we write $Wh(f)$.

The following lemma appears in [Roeder et al. 07]:

Lemma 2.4. *Let the abstract polyhedron C' be obtained from the simple abstract polyhedron C by a Whitehead move $Wh(e)$. Then if $\mathcal{P}^0_C$ is nonempty, so is $\mathcal{P}^0_{C'}$.*

The proof constructs a sequence of polyhedra realizing C with dihedral angles chosen such that the edge e converges to a single point at infinity. A carefully chosen small perturbation of this limiting configuration results in a compact polyhedron realizing C' with nonobtuse dihedral angles.

Suppose that we have a polyhedron realizing C with all dihedral angles equal to $\frac{2\pi}{5}$, and choose a small $\epsilon > 0$. To implement a Whitehead move using the computer, we assign the dihedral angle ϵ to the edge e and dihedral angle $\frac{\pi}{2}$ to the four edges sharing an endpoint with e.

With the dihedral angles of the remaining edges left the same, the resulting set of angles is in A_C, and hence we can use Newton's method to deform P into a polyhedron P_1 realizing C with these new angles.

If ϵ was chosen small enough, P_1 will be in the basin of attraction for a polyhedron realizing C' with the edge e' replacing e, the dihedral angle at e' equal to ϵ, and all other dihedral angles as in P_1. We call the resulting polyhedron P_2. Since C' is simple, we can deform P_2 to have all dihedral angles $\frac{2\pi}{5}$, and so we obtain P'.

Figure 7 shows these four steps during a Whitehead move on one of the edges of the dodecahedron. Here and elsewhere in this paper we use $\epsilon \approx 0.02$. (A smaller ϵ may be necessary in constructing polyhedra with a very large number of faces.)

If we can find a sequence of combinatorial Whitehead moves reducing a given simple abstract polyhedron C to either Pr_N or D_N via a sequence of simple abstract polyhedra $C_1, \ldots, C_N$, we can use Newton's method to perform this sequence of Whitehead moves in the reverse order, constructing geometric polyhedra that realize $C_N, C_{N-1}, \ldots, C_1$, and finally C. Before explaining why such a sequence always exists, we demonstrate this process for the dodecahedron.

In Figure 8 we show a sequence of Whitehead moves reducing the dodecahedron to D_{12}, carefully avoiding intermediate abstract polyhedra that contain prismatic 3-circuits.

Working backward through this sequence from D^*_{12} to the dodecahedron, we obtain the following sequence of Whitehead moves: $Wh(8, 11)$, $Wh(4, 11)$, $Wh(1, 2)$,

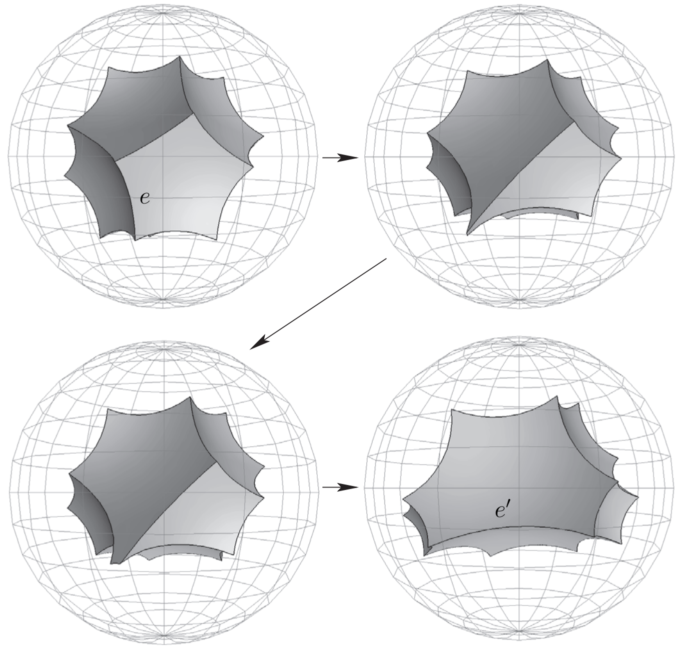

FIGURE 7. Whitehead move $Wh(e)$ on edge e of the dodecahedron.

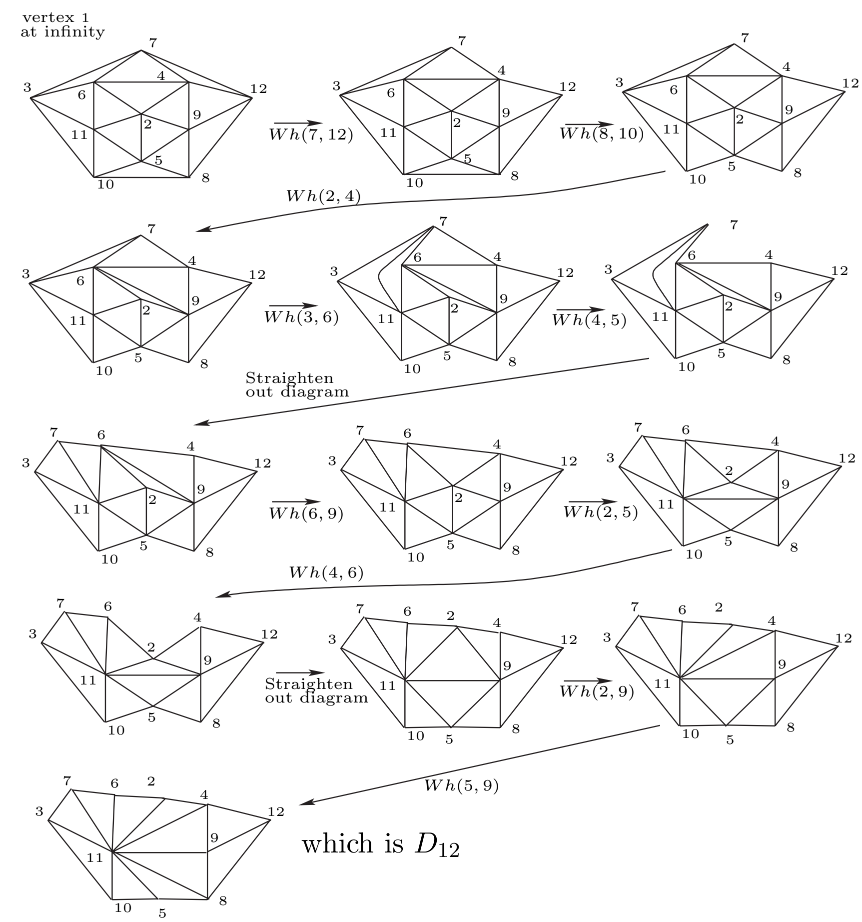

FIGURE 8. Choosing a sequence of Whitehead moves to reduce the dodecahedron to D_{12}, while avoiding prismatic 3-circuits.

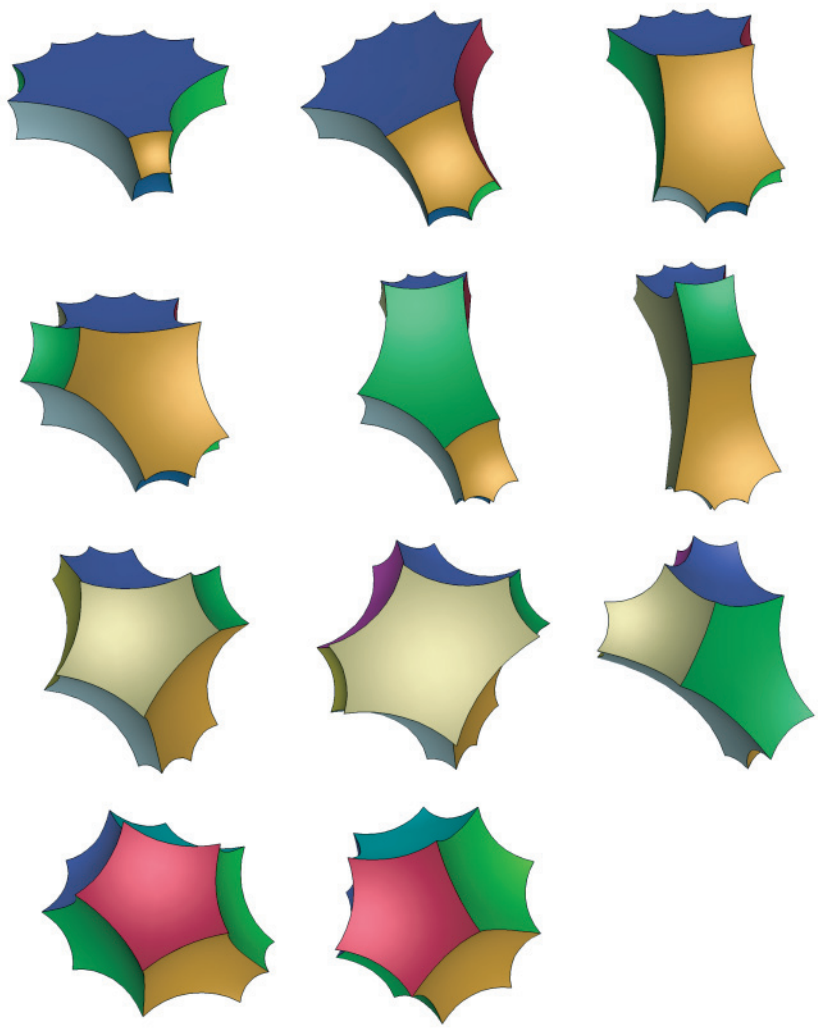

FIGURE 9. Construction of the dodecahedron from D_{12} by "undoing" the ten Whitehead moves shown in Figure 8.

$Wh(9,11)$, $Wh(2,4)$, $Wh(1,6)$, $Wh(7,11)$, $Wh(6,9)$, $Wh(1,5)$, and $Wh(1,4)$.

Starting with D_{12}, we use Newton's method to perform each of these Whitehead moves geometrically, obtaining the dodecahedron as the end result. Figure 9 shows D_{12} in the upper-left corner, the dodecahedron at the bottom center, and each of the intermediate polyhedra obtained in this process in between, ordered left to right, top to bottom.

2.6 A Lemma on Whitehead Moves

The following lemma from [Andreev 70a] and [Roeder et al. 07] is necessary to prove Andreev's theorem and for our construction of simple polyhedra performing Whitehead moves geometrically with Newton's method.

Lemma 2.5. (Whitehead sequence.) *Let C be a simple abstract polyhedron on $\mathbb{S}^2$ that is not a prism. If C has $N > 7$ faces, C can be simplified to D_N by a finite sequence of Whitehead moves such that all of the intermediate abstract polyhedra are simple.*

Theorem 6 in Andreev's original paper contains our Lemma 2.5. Andreev's original proof of Theorem 6 provides an algorithm to produce the Whitehead moves needed for this lemma, but the algorithm contains a glitch. The error was detected when the algorithm was implemented for the computer program described in this paper and tested on the first example, the dodecahedron.

Instead of using $Wh(6,9)$ for the fifth Whitehead move of the sequence described in the previous section, Andreev's algorithm uses either $Wh(2,6)$ or $Wh(2,5)$. In

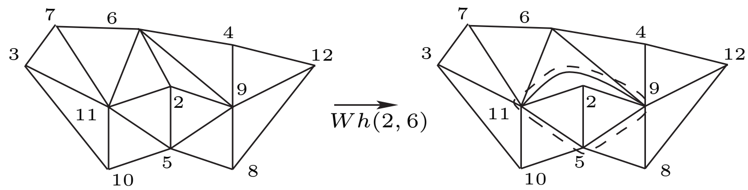

FIGURE 10. Creating a prismatic 3-circuit using Andreev's algorithm.

both cases it produces an abstract polyhedron that has a prismatic 3-circuit; see Figure 10.

In combination with the computer-implemented Whitehead move described in the previous section, the sequence of Whitehead moves given in the proof of Lemma 2.5 gives us the path that we will use for our homotopy method in constructing simple polyhedra. We provide an outline of the proof here that is sufficient to describe the sequence of Whitehead moves. Those who wish to see a complete proof may refer to [Roeder et al. 07, Roeder 04].

2.6.1 Outline of the Proof of Lemma 2.5.

We assume that $C \neq \mathrm{Pr}_N$ is a simple abstract polyhedron with $N > 7$ faces. We will construct a sequence of Whitehead moves that change C to D_N, so that no intermediate complex has a prismatic 3-circuit.

Find a vertex v_∞ of C^* that is connected to the greatest number of other vertices. We will call the link of v_∞, a cycle of k vertices and k edges, the *outer polygon*. Most of the work is to show that we can do Whitehead moves to increase k to $N-3$ without introducing any prismatic 3-circuits during the process. Once this is completed, it is easy to change the resulting complex to D_N^* by additional Whitehead moves.

Let us set up some notation. Draw the dual complex C^* in the plane with the vertex v_∞ at infinity and the outer polygon P surrounding the remaining vertices and triangles, as in Figure 11. We call the vertices inside of P *interior vertices*. All of the edges inside of P that do not have an endpoint on P are called *interior edges*.

Note that the graph of interior vertices and edges is connected, since C^* is simple. An interior vertex that is connected to only one other interior vertex will be called an *endpoint*.

Throughout this proof we will draw P and the interior edges and vertices of C^* in black. The connections between P and the interior vertices will be gray. Connections between P and v_∞ will be black, if shown at all.

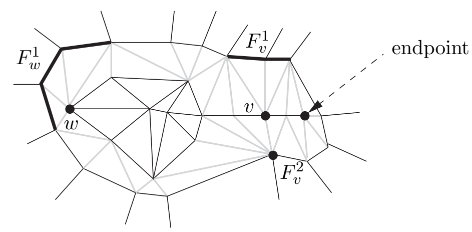

FIGURE 11. Illustration of the terms *outer polygon*, *interior vertices*, *interior edges*, and *endpoint*.

The link of an interior vertex v intersects P in a number of components $F_v^1, \ldots, F_v^n$ (possibly $n = 0$). See Figure 11 for an example. We say that v is *connected to P in these components*. Notice that since C^* is simple, an endpoint is always connected to P in exactly one such component.

Move 1. Suppose that there is an interior vertex A of C^* that is connected to P in exactly one component consisting of exactly two consecutive vertices Q and R. The Whitehead move $Wh(QR)$ on C^* increases the length of the outer polygon by one, and introduces no prismatic 3-circuit.

Move 2. Suppose that there is an interior vertex A that is connected to P in a component consisting of M consecutive vertices $Q_1, \ldots, Q_M$ of P (and possibly other components).

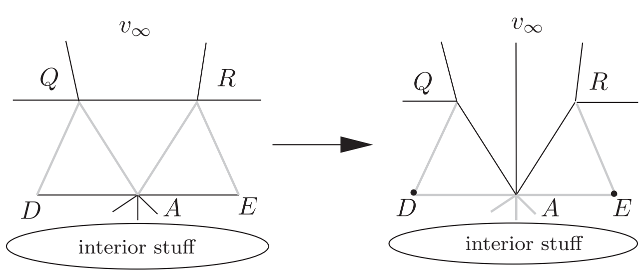

FIGURE 12. Move 1.

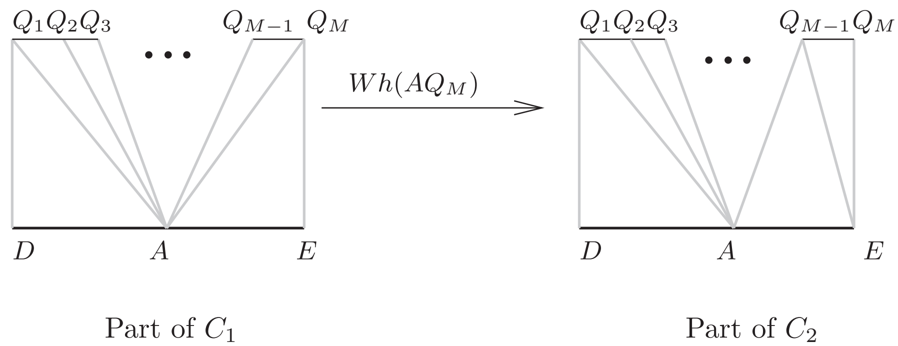

FIGURE 13. Move 2 part (a).

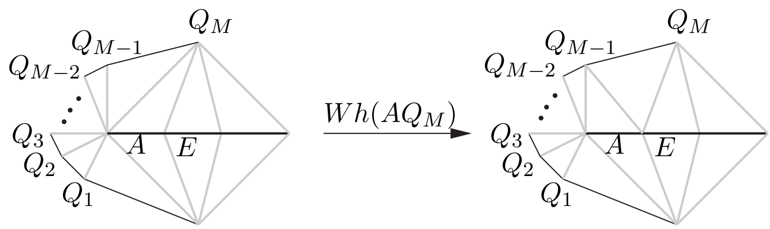

FIGURE 14. Move 2 part (b).

(a) If A is not an endpoint and $M > 2$, the sequence of Whitehead moves $Wh(AQ_M), \ldots, Wh(AQ_3)$ results in a complex in which A is connected to the same component of P in only Q_1 and Q_2. These moves leave P unchanged, and introduce no prismatic 3-circuit.

(b) If A is an endpoint and $M > 3$, the sequence of Whitehead moves $Wh(AQ_M), \ldots, Wh(AQ_4)$ results in a complex in which A is connected to the same component of P in only Q_1, Q_2, and Q_3. These moves leave P unchanged and introduce no prismatic 3-circuits.

Note 2.6. In both parts (1) and (2), each of the Whitehead moves $Wh(AQ_M)$ transfers the connection between A and Q_M to a connection between the neighboring interior vertex E and Q_{M-1}. This is helpful in case 2 later.

Move 3. Suppose that there is an interior vertex A whose link contains two distinct vertices X and Y of P. Then there are Whitehead moves that eliminate any component in which A is connected to P if that component does not contain X or Y. Then P is unchanged, and no prismatic 3-circuits will be introduced.

In Figure 15, A is connected to P in four components containing six vertices. We can eliminate connections of A to all of the components except for the single-point components X and Y.

The proof that this move does not introduce any new prismatic 3-circuit is rather technical and depends essentially on the fact that A is connected to P in at least two other vertices X and Y. Andreev describes a nearly identical process to Move 3 in [Andreev 70a, pp. 333–334]. However, he merely assumes that A is connected to P in at least one component in addition to the components being eliminated. He does not require that A be connected to P in at least two vertices outside of the components being eliminated. Andreev then asserts, "It is readily seen that all of the polyhedra obtained in this way are simple. . . ." In fact, the Whitehead move demonstrated in Figure 10 creates a prismatic 3-circuit.

Having assumed this stronger (and incorrect) version of Move 3, the remainder of Andreev's proof is relatively

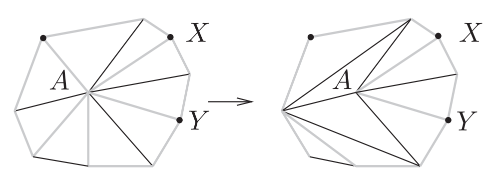

FIGURE 15. Move 3.

easy. Unfortunately, the situation pictured in Figure 10 is not uncommon (as we will see in Case 3 below). Restricted to the weaker hypotheses of Move 3, we will have to work a little bit harder.

Using Moves 1, 2, and 3, we check that if the length of P is less than $N-3$, then there is a sequence of Whitehead moves that increases the length of P by 1 without introducing any prismatic 3-circuits.

Case 1: An interior vertex that is not an endpoint connects to P in a component with two or more vertices, and possibly in other components.

Apply Move 2, decreasing this component to two vertices. We can then apply Move 3, eliminating any other components, since this component contains two vertices. Finally, apply Move 1 to increase the length of the outer polygon by 1.

Case 2: An interior vertex that is an endpoint is connected to more than three vertices of P.

We assume that each of the interior vertices that are not endpoints are connected to P in components consisting of single vertices; otherwise, we are in Case 1.

Let A be the endpoint that is connected to more than three vertices of P. By Move 2, part (2), there is a Whitehead move that transfers one of these connections to the interior vertex E that is next to A. Now one of the components in which E is connected to P has exactly two vertices. The vertex E is not an endpoint, since $k < N-3$ implies that there are at least three interior vertices. Once this is done, we can apply Case 1.

Case 3: Each interior vertex that is an endpoint is connected to exactly three vertices of P, and each interior vertex that is not an endpoint is connected to P in components each consisting of a single vertex.

First, notice that if the interior vertices and edges form a line, the restriction on how interior vertices are connected to P results in the prism, contrary to the assumption that C is not the prism. However, there are many complexes satisfying the hypotheses of this case that have interior vertices and edges forming a graph more complicated than a line; see Figure 16 for an example.

For such complexes we need a very special sequence of Whitehead moves to increase the length of P.

Pick an interior vertex that is an endpoint and label it I_1. Denote by P_1, P_2, and P_3 the three vertices of P to which I_1 connects. Then I_1 will be connected to a sequence of interior vertices $I_2, I_3, \ldots, I_m$, with $m \geq 2$, with I_m the first interior vertex in the sequence that is connected to more than two other interior vertices. Vertex I_m must exist by the assumption that the interior

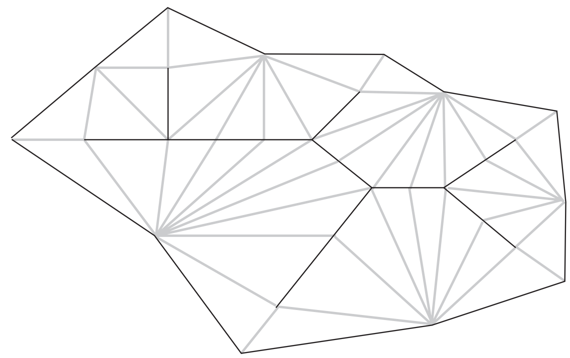

FIGURE 16. A (complicated) abstract polyhedron for which Case 3 is necessary. See Section 2.7 for a simpler example.

vertices do not form a line segment, the configuration that we ruled out above. By hypothesis, $I_2, \ldots, I_m$ can connect to P only in components each of which consists of a vertex; hence each must be connected to P_1 and to P_3. Similarly, there is an interior vertex (call it X) that connects to both I_m and P_1 and another vertex Y that connects to I_m and P_3. Vertex I_m may connect to other vertices of P and other interior vertices, as shown on the left side of Figure 17.

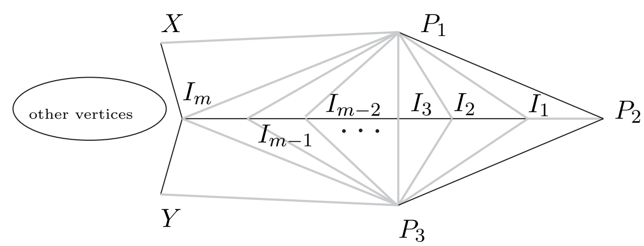

FIGURE 17. Initial configuration for Case 3.

Now we describe a sequence of Whitehead moves that can be used to connect I_m to P in only P_1 and P_2. This will allow us to use Move 1 to increase the length of P by 1.

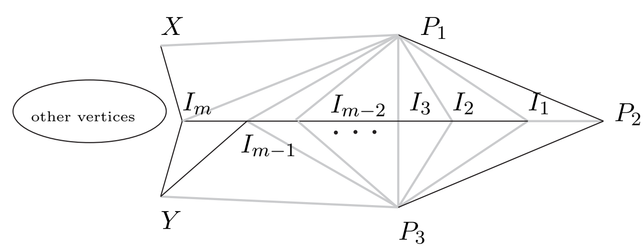

FIGURE 18. Configuration after eliminating all connections of I_m to P, except for P_1.

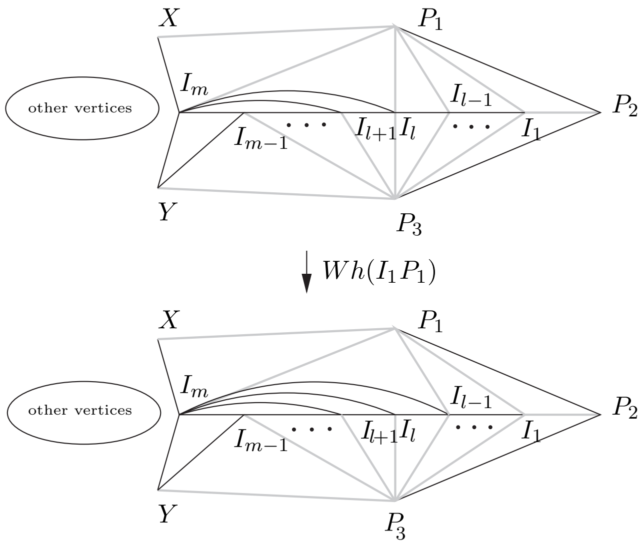

FIGURE 19. Application of move $Wh(I_1P_1)$.

First, using Move 3 we can eliminate all possible connections of I_m to P in places other than P_1 and P_3. Next, we do the move $Wh(I_mP_3)$ so that I_m connects to P only in P_1.

Next, we must do the moves $Wh(I_{m-1}P_1), \ldots, Wh(I_1P_1)$, in that order (see Figure 19).

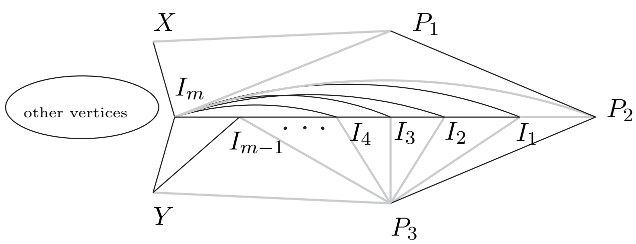

FIGURE 20. Configuration after I_m is connected to precisely the two vertices P_1 and P_2 on P.

After this sequence of Whitehead moves we obtain Figure 20, with I_m connected to P exactly at P_1 and P_2, so that we can apply Move 1 to increase the length of P by the move $Wh(P_1P_2)$, as shown in Figure 21.

This concludes Case 3.

Since C^* must belong to one of these cases, we have seen that if the length of P is less than $N-3$, we can do Whitehead moves to increase it to $N-3$ without creating prismatic 3-circuits. Hence we can reduce to the case of two interior vertices, both of which must be endpoints. Then we can apply Move 2 part (b) to decrease the number of connections between one of these two interior vertices and P to exactly 3. The result is the complex D_N, as shown to the right in Figure 22.

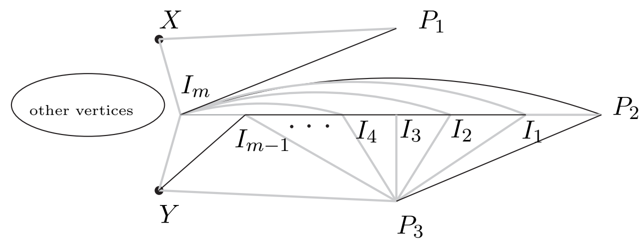

FIGURE 21. Configuration after Case 3 is completed.

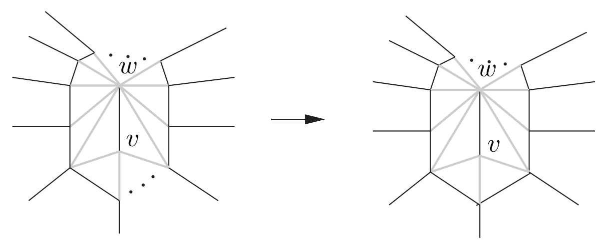

FIGURE 22. Final Whitehead moves after increasing the length of the outer polygon to $N-3$.

2.7 Construction of a "Difficult" Simple Polyhedron

In Figures 23, 24, and 25 we illustrate the algorithm described in the previous section by constructing a hyperbolic polyhedron for which Case 3 from the proof of Lemma 2.5 is necessary. (The rather astute reader may also notice an alternative method of construction by stacking three prisms with appropriately chosen dihedral angles. To the author's knowledge, this cannot be done for all polyhedra for which Case 3 is required.)

Following the Whitehead moves backward from D_{18}^* to R_{18}^*, we obtain the following sequence of Whitehead moves:

$Wh(6,13)$, $Wh(6,9)$, $Wh(3,6)$, $Wh(9,18)$, $Wh(6,15)$, $Wh(6,16)$, $Wh(6,17)$, $Wh(6,7)$, $Wh(6,8)$, $Wh(6,4)$, $Wh(8,18)$, $Wh(7,9)$, $Wh(9,14)$, $Wh(9,15)$, $Wh(3,18)$, $Wh(7,8)$, $Wh(4,18)$, $Wh(3,8)$, $Wh(8,9)$, $Wh(5,18)$, $Wh(4,9)$, $Wh(6,9)$, $Wh(2,18)$, $Wh(5,6)$, $Wh(1,18)$, $Wh(1,13)$, $Wh(1,3)$, $Wh(3,4)$, $Wh(4,5)$, $Wh(2,5)$.

We performed this sequence of Whitehead moves geometrically, using Newton's method. The result, starting with D_{18} and realizing R_{18}, is shown in Figure 26. Each polyhedron is displayed in the conformal ball model.

2.8 Truncation of Vertices

We have seen an outline of how to construct simple polyhedra. We now show how to construct all truncated polyhedra except for the triangular prism, which we have already constructed in Section 2.5.

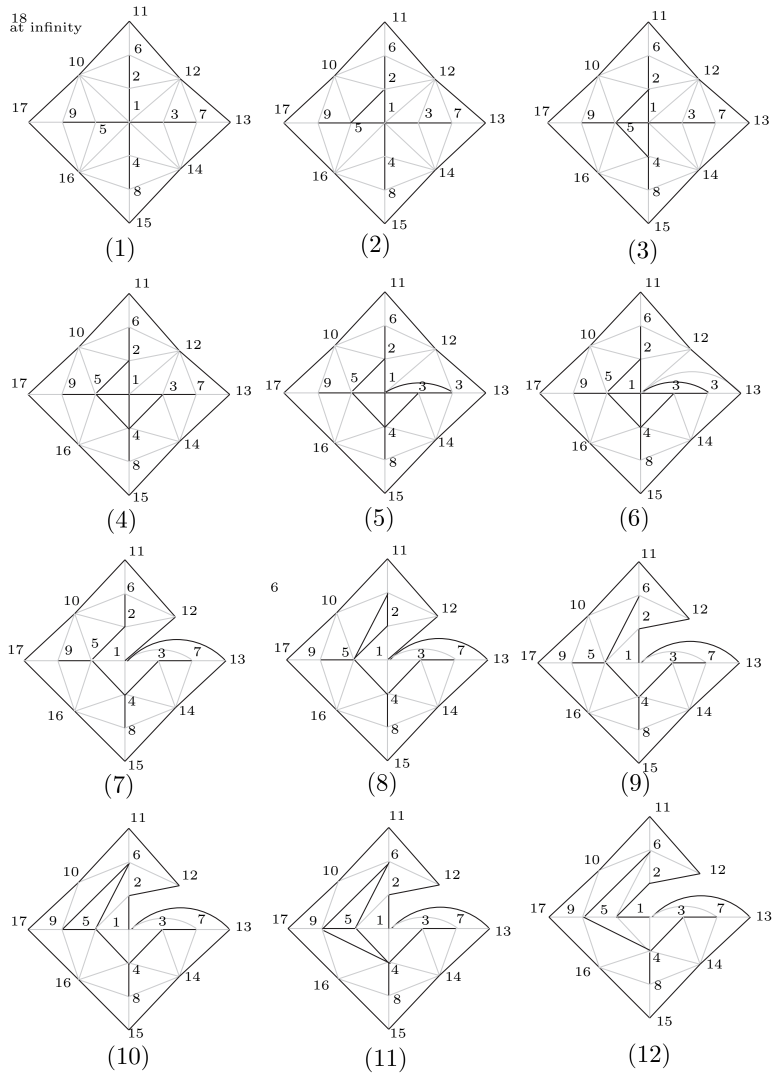

FIGURE 23. Case 3 from the proof of Lemma 2.5 is done in pictures (1)–(7). Case 1 follows in pictures (7)–(9) and again (for a different edge of P) in pictures (9)–(12).

Lemma 2.7. *If $A_C \neq \varnothing$, then there are points in A_C arbitrarily close to $(\pi/3, \pi/3, \ldots, \pi/3)$.*

Proof: Simply check that if $\mathbf{a} \in A_C$, then the entire straight-line path to $(\pi/3, \pi/3, \ldots, \pi/3)$, excluding the final point, is in A_C. □

Thus we can assume that $\mathbf{a}$ is arbitrarily close to $(\pi/3, \pi/3, \ldots, \pi/3)$, because once we have a polyhedron realizing C with nonobtuse dihedral angles, we can deform it to have any dihedral angles in A_C, as described in Section 2.4. Specifically, choose some $0 < \delta < \frac{\pi}{18}$ and assume that each component of $\mathbf{a}$ is within δ of $\frac{\pi}{3}$.

Let $\widetilde{C}$ be the modification of C obtained by replacing each of the triangular faces f_i^{tr} by a single vertex v_i^{tr}. (Or if C is the truncated triangular prism, let $\widetilde{C}$ be the prism.) Let $\hat{\mathbf{a}}$ be the angles from $\mathbf{a}$ corresponding to the edges from C that are in $\widetilde{C}$, and let $\beta = (\hat{\mathbf{a}}_1 + 2\delta, \hat{\mathbf{a}}_2 + 2\delta, \ldots)$. If $\widetilde{C}$ is the prism, renumber the edges so that the three edges forming the prismatic cycle are the first three, and choose

$$\beta = (\hat{\mathbf{a}}_1, \hat{\mathbf{a}}_2, \hat{\mathbf{a}}_1, \hat{\mathbf{a}}_5 + 2\delta, \hat{\mathbf{a}}_5 + 2\delta, \ldots).$$

Note that δ was chosen so that $\beta \in A_{\widetilde{C}}$. Then, the straight-line path $\mathbf{a}(t)$ joining β to $\hat{\mathbf{a}}$ (parameterized by $t \in (0,1)$) will remain in $A_{\widetilde{C}}$, except that the sum of the dihedral angles of edges meeting at each of the vertices v_i^{tr} will decrease past π at some time $t_i \in (0,1)$.

In [Roeder et al. 07, Roeder 04] the authors use the path $\mathbf{a}(t)$ to construct a sequence of polyhedra $\widetilde{P} =$

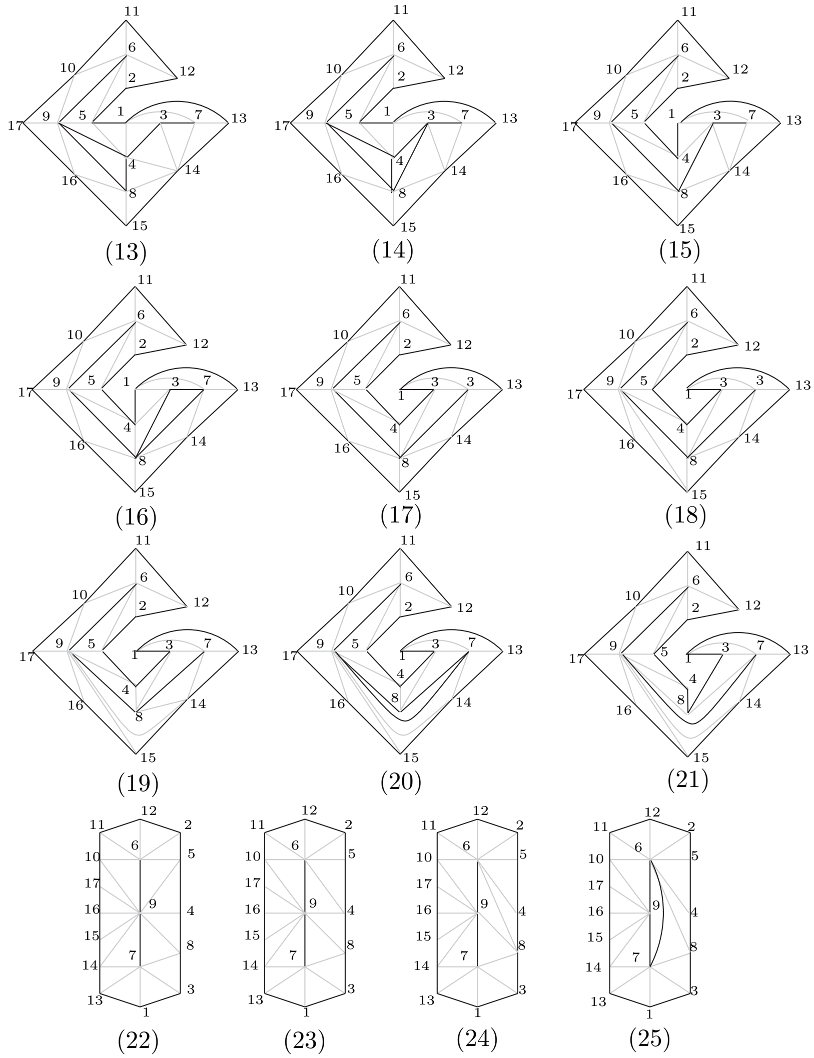

FIGURE 24. Continuing from Figure 23. Case 1 is repeated three times in pictures (12)–(15), then in (15)–(17), and finally in (17)–(21). The figure is straightened out between pictures (21) and (22), and then Case 1 is done in (22)–(29).

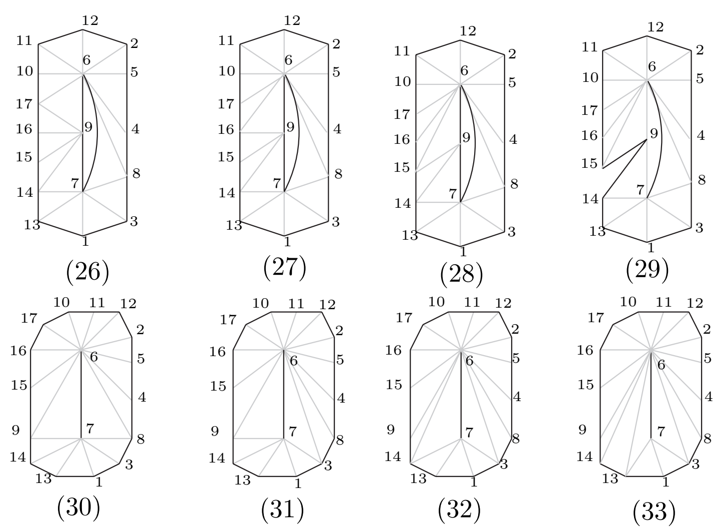

FIGURE 25. Continuing from Figure 24. Pictures (22)–(29) are another instance of Case 1. The figure has been straightened out between pictures (29) and (30). A sequence of final Whitehead moves is done in pictures (30)–(33), so that one of the two interior vertices is connected to only three points on the outer polygon. This reduces the complex to D_{18}^{*}.

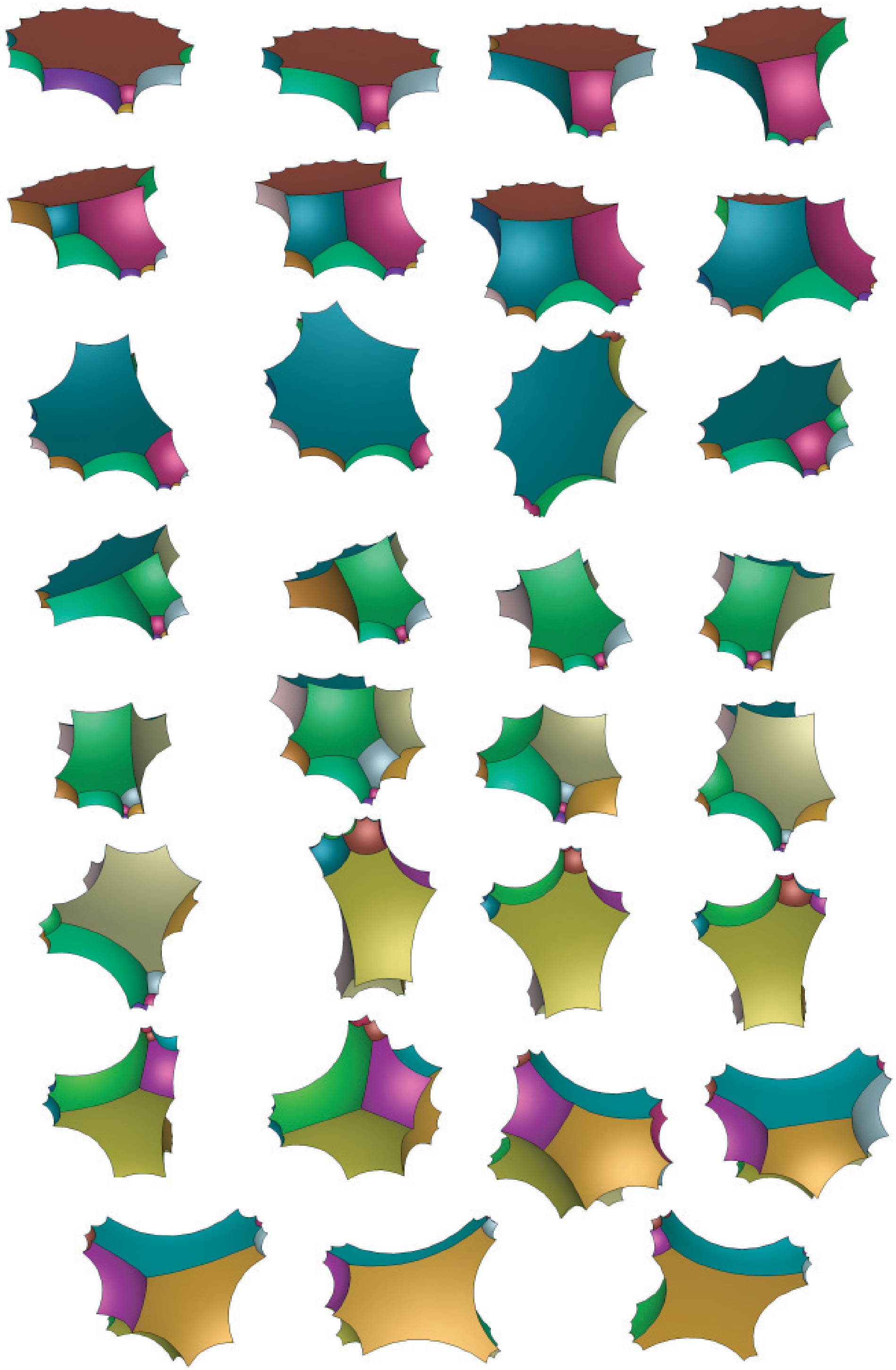

FIGURE 26. Construction of R_{18} from D_{18} using 30 Whitehead moves.

$P_0, P_1, \ldots, P_{N-1} = P$, where $\widetilde{P}$ realizes C, and P_i is obtained from P_{i-1} by truncating the vertices that become ideal when $t = t_i$. Realizing P proves that $\mathcal{P}_C^0 \neq \varnothing$, as needed for the proof of Andreev's theorem.

Because the proof from [Roeder et al. 07, Roeder 04] gives us a priori knowledge that compact polyhedra exist that realize each of the intermediate combinatorial structures, we can use Newton's method to deform the planes

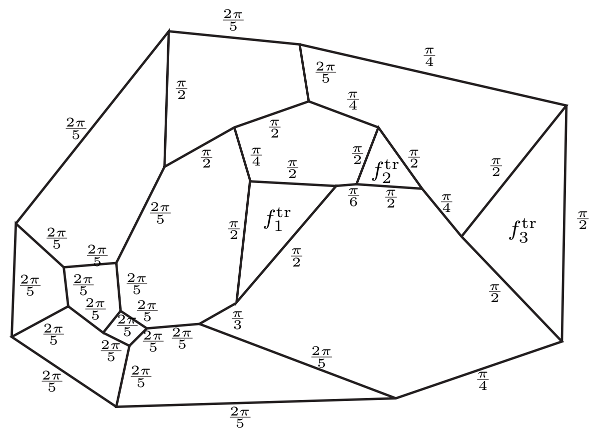

FIGURE 27. Specification for a polyhedron with three triangular faces (corresponding to truncated vertices). These faces are labeled f_1^{tr}, f_2^{tr}, and f_3^{tr}.

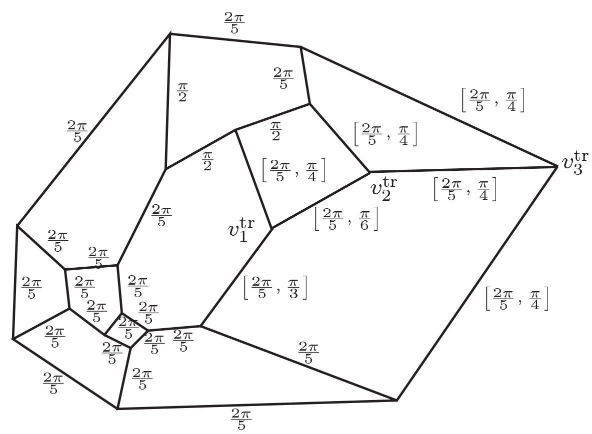

FIGURE 28. Deformation of dihedral angles necessary to realize the polyhedron from Figure 27.

forming $\widetilde{P}$ to realize the angles in the entire path $\mathbf{a}(t)$ without truncating each vertex once it meets $\partial_\infty \mathbb{H}^3$. We can then solve independently for the planes corresponding to the triangles in C so that each intersects the three appropriate planes at the three appropriate angles.

We illustrate this construction for the pair $(C, \mathbf{a})$ shown in Figure 27, which has three truncations, labeled f_1^{tr}, f_2^{tr}, and f_3^{tr}.

The path $\mathbf{a}(t)$ described above works with any truncated C. For many C, such as the current one, a much easier path $\mathbf{a}(t)$ can be found satisfying conditions (1), (3), (4), and (5) from Andreev's theorem for $\widetilde{C}$, but for which the sum of the dihedral angles of the edges meeting at each v_i^{tr} decreases past π at some $t_i \in (0,1)$. Such a path is sufficient for our construction. For the current construction, $\widetilde{C}$ is shown in Figure 28, with edges labeled according to an appropriate path $\mathbf{a}(t)$. (Notation: $\mathbf{a}(t) = \beta$ for the edges labeled with a single angle β, whereas $\mathbf{a}(t) = \eta(1-t) + \gamma t$ for the edges $[\eta, \gamma]$.)

We constructed a polyhedron $\widetilde{P}$ realizing the pair $(\widetilde{C}, \mathbf{a}(0))$ and used Newton's method to deform the faces so that the dihedral angles follow the path $\mathbf{a}(t)$. After obtaining a noncompact polyhedron $\widetilde{P}_1$ realizing angles $\mathbf{a}(1)$, we truncated the vertices $v_1^{\mathrm{tr}}, v_2^{\mathrm{tr}}, v_3^{\mathrm{tr}}$. The final re-

FIGURE 29. Realization of the abstract polyhedron and choice of dihedral angles from Figure 27.

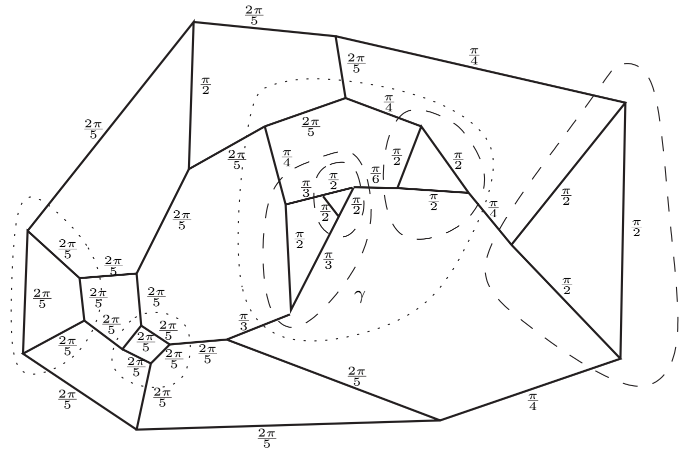

FIGURE 30. A compound abstract polyhedron C and choice of dihedral angles satisfying conditions (1)–(5) from Andreev's theorem.

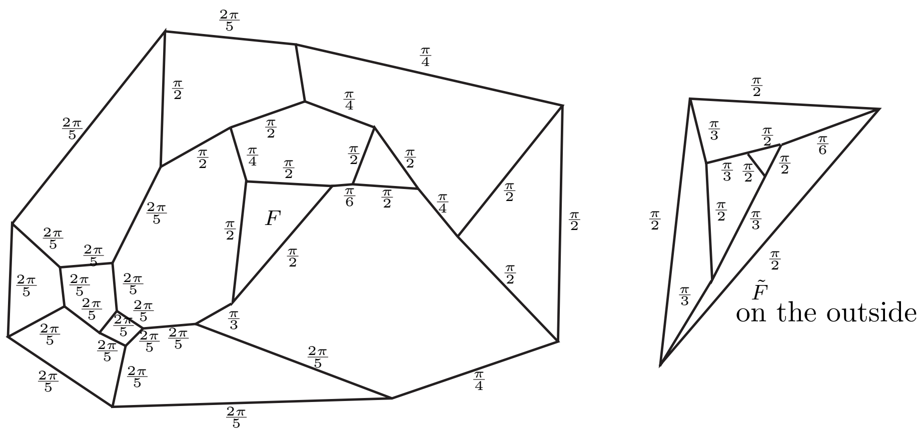

FIGURE 31. Cutting C along the 3-circuit γ, obtaining two abstract polyhedra.

sult is the polyhedron shown in Figure 29, which will be used in the next section to form part of a compound polyhedron.

2.9 Constructing Compound Polyhedra

Any compound polyhedron can be constructed by gluing together a finite number of truncated polyhedra. We illustrate this construction for the polyhedron shown in Section 1.2 and repeated here in Figure 30.

In general, one cuts along every prismatic 3-circuit that does not correspond to a triangular face. Here there is one such circuit, which is labeled γ. We cut along γ, obtaining the two combinatorial polyhedra depicted in Figure 31, for which every prismatic 3-circuit corresponds to a triangular face.

In this case, the diagram on the left of Figure 31 is that for the polyhedron that we constructed in the previous section. The diagram on the right side of Figure 31 is that of the truncated triangular prism, which can also be easily constructed.

We require that the new triangular faces F and $\widetilde{F}$ obtained by cutting along γ be perpendicular to each of the other faces that they intersect. Then each face angle

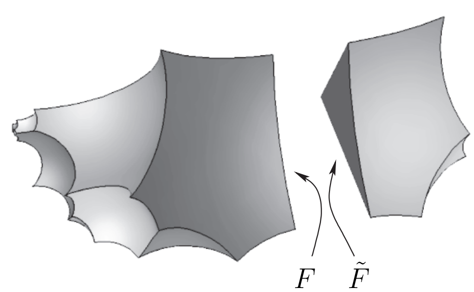

FIGURE 32. Geometric realization of the abstract polyhedra depicted in Figure 31.

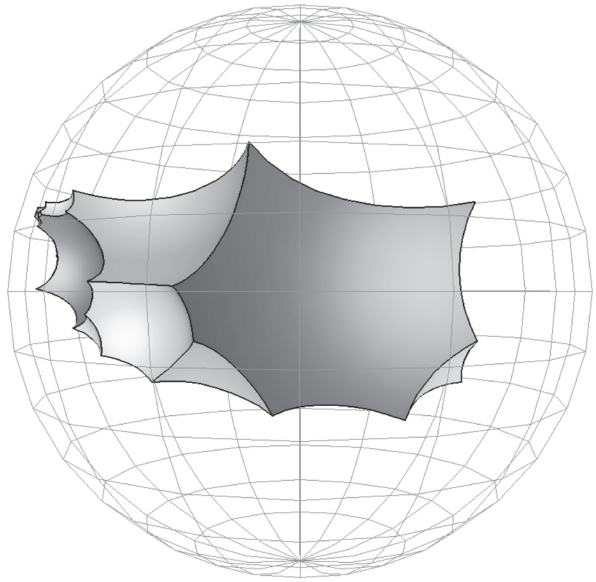

FIGURE 33. Geometric realization of the abstract polyhedron depicted in Figure 30, obtained by gluing faces F to $\tilde{F}$ from the two polyhedra from Figure 32.

equals the dihedral angle outside of F, or $\widetilde{F}$, that leads to that vertex. Because we obtained the two diagrams by cutting the original diagram along γ, the dihedral angles on the edges leading to F and $\widetilde{F}$ are the same, and we naturally obtain that F and $\widetilde{F}$ have the same face angles, but are mirror images of each other.

These two polyhedra glue perfectly together to form a polyhedron realizing $(C, \mathbf{a})$ as shown in Figure 33.

3. APPLICATIONS TO DISCRETE GROUPS AND POLYHEDRAL ORBIFOLDS

Let P be a finite-volume hyperbolic polyhedron having dihedral angles each of which is a proper integer submultiple of π. It is a well-known application of the Poincaré polyhedron theorem [Poincaré 83] that the group generated by reflections in the faces of P forms a discrete subgroup Γ_P of $\mathrm{Isom}(\mathbb{H}^3)$. Such groups have been extensively studied; see [Vinberg 85] and the references therein.

Given such a discrete reflection group Γ_P, we denote the corresponding orbifold by $O_P = \mathbb{H}^3/\Gamma_P$. We will use the term *polyhedral orbifolds* to describe orbifolds obtained in this way. (Note: often in the literature, the term "polyhedral orbifold" is used to describe the oriented double cover $\mathbb{H}^3/\Gamma_P^+$, where Γ_P^+ is the index-two subgroup consisting of orientation-preserving elements of Γ_P.) See [Thurston 80, Chapter 13] and [Reni 97] for more details on polyhedral orbifolds.

We use the computer program described in this paper to construct examples from three classes of polyhedral orbifolds: the Lambert cubes [Kellerhals 89], the Löbell orbifolds [Löbell 31, Vesnin 87, Mednykh and Vesnin 03], and a mysterious orbifold described in [Mednykh and Vesnin 03] whose 16-fold cover is a "hyperelliptic" compact hyperbolic manifold.

We output the generators of each reflection group as elements of $\mathrm{SO}(3,1)$ into SnapPea, computing volumes and length spectra of these orbifolds. For details on how SnapPea calculates the length spectrum, refer to [Hodgson and Weeks 94].

Note 3.1. Only after doing the experiments in this section did the author discover Damian Heard's program Orb. Using the currently available version of Orb, it was easy to construct and study orbifold double covers of the Lambert cubes, but the author failed to construct those corresponding to Löbell polyhedra and the Mednykh–Vesnin polyhedron. Using the currently available version of Orb, it was possible to construct and study orbifold double covers for each of the orbifolds considered in this section.

3.1 Construction of Lambert Cubes

A Lambert cube is a compact polyhedron realizing the combinatorial type of a cube, with three noncoplanar, nonadjacent edges chosen and assigned dihedral angles

$O_{\text{Lambert}}(3,3,3)$	Computed Volume: 0.324423	Theoretical Volume: 0.3244234492
Short Geodesics	6 mI 1.087070	3 mI $1.087070 + i \cot 2\pi/3$
	6 mI 1.400257	6 mI $1.400257 + i \cdot \pi$
	3 mI $1.601733 + i \cdot 2.765750$	3 mI $1.790480 + i \cdot 0.762413$
	6 mI 1.864162	3 mI 2.138622
	4 mI 2.174140	6 mI $2.199243 + i \cdot 2.436822$
$O_{\text{Lambert}}(3,4,5)$	Computed Volume: 0.479079	Theoretical Volume: 0.4790790206
Short Geodesics	2 mI 0.622685	1 mI $0.622685 + i \cdot 1.256637$
	1 mI $0.622685 + i \cdot 2.513274$	3 mI 0.883748
	1 mI $0.883748 + i \cdot 1.570797$	1 mI $0.883748 + i \cdot \pi$
	1 mI 1.123387	1 mI $1.123387 + i \cdot \pi$
	1 mI 1.245371	
$O_{\text{Lambert}}(4,4,4)$	Computed Volume: 0.554152	Theoretical Volume: 0.5382759501
Short Geodesics	2 mI 0.175240	1 mI $0.175240 + i \cdot 0.369599$
	1 mI $0.175240 + i \cdot 1.108797$	1 mI $0.175240 + i \cdot 0.739198$
	1 mI $0.175240 + i \cdot 0.739198$	1 mI $0.175240 + i \cdot 1.478396$
	1 mI $0.175240 + i \cdot 1.847996$	1 mI $0.175240 + i \cdot 2.217595$
	1 mI $0.175240 + i \cdot 2.587194$	1 mI $0.175240 + i \cdot 2.956793$
	1 mI 0.350479	
$O_{\text{Lambert}}(5,8,12)$	Computed Volume: 0.768801	Theoretical Volume: 0.7688005863
Short Geodesics	3 mI 0.407809	1 mI $0.407809 + i \cdot 0.523599$
	1 mI $0.407809 + i \cdot 1.047198$	1 mI $0.407809 + i \cdot 1.570797$
	1 mI $0.407809 + i \cdot 2.094396$	1 mI $0.407809 + i \cdot 2.617995$
	1 mI $0.407809 + i \cdot \pi$	2 mI 0.643110
	1 mI $0.643110 + i \cdot 0.785398$	1 mI $0.643110 + i \cdot 1.570796$
	1 mI $0.643110 + i \cdot 2.356194$	1 mI $0.643110 + i \cdot \pi$

TABLE 1. Volumes and length spectra for Lambert cubes.

α, β, and γ, and the remaining edges assigned dihedral angles $\frac{\pi}{2}$. It is easy to verify that if $0 < \alpha, \beta, \gamma < \frac{\pi}{2}$, then such an assignment of dihedral angles satisfies the hypotheses of Andreev's theorem. The resulting polyhedron is called the (α, β, γ) Lambert cube, which we will denote by $P_{\alpha,\beta,\gamma}$. Thus, there are discrete reflection groups generated in the faces of a Lambert cube when $\alpha = \frac{\pi}{p}$, $\beta = \frac{\pi}{q}$, and $\gamma = \frac{\pi}{r}$ for integers $p, q, r > 2$. We denote the corresponding orbifold by $O_{\text{Lambert}}(p, q, r)$. In Table 1, we present volumes and the lengths of the shortest geodesics for a sampling of Lambert cubes for small p, q, and r.

The format of the lists of geodesic lengths presented in this and in the following tables is the same as that presented by SnapPea. The first entry is the multiplicity of distinct geodesics having the same complex length. The second entry either is "mI," to indicate that the geodesic has the topological type of a mirrored interval, or else is empty if the geodesic has the topological type of a circle. The third entry is the complex length. Nearly all of the short geodesics that we present in these tables are mirrored intervals, because our orbifolds are mirrored polyhedra and because we have listed only rather short geodesics.

Also notice that while SnapPea provides many more digits of precision for the geodesic length than we have used, we have rounded to the first six decimal places in order to group geodesics that are likely to correspond to the same class but weren't listed that way due to numerical imprecision.

The volumes of Lambert cubes have been explicitly calculated by R. Kellerhals [Kellerhals 89]. If we write $\Delta(\eta, \xi) = \Lambda(\eta + \xi) - \Lambda(\eta - \xi)$, where Λ is the well-known Lobachevsky function $\Lambda(x) = -\int_0^x \log|2\sin(t)|dt$, then

$$\begin{aligned}\mathrm{Vol}(P_{\alpha,\beta,\gamma}) = \frac{1}{4}\Big(&\Delta(\alpha,\theta) + \Delta(\beta,\theta) + \Delta(\gamma,\theta) \\ &- 2\cdot\Delta\left(\frac{\pi}{2},\theta\right) - \Delta(0,\theta)\Big), \qquad (3\text{–}1)\end{aligned}$$

where θ, with $0 < \theta < \frac{\pi}{2}$, is the parameter defined by

$$\tan^2(\theta) = p + \sqrt{p^2 + L^2M^2N^2},$$
$$p = \frac{L^2 + M^2 + N^2 + 1}{2},$$

and

$$L = \tan\alpha, \quad M = \tan\beta, \quad N = \tan\gamma.$$

The column in Table 1 labeled "computed volume" gives the volume of $O_{\text{Lambert}}(p, q, r)$ as computed using SnapPea, while the column labeled "theoretical volume" gives the volume of $O_{\text{Lambert}}(p,q,r)$ computed using (3–1).

3.2 Construction of Löbell Orbifolds

For each $n > 5$, there is a radially symmetric combinatorial polyhedron having two n-sided faces and $2n$ faces with five sides, which provides a natural generalization of the dodecahedron. This combinatorial polyhedron is depicted in Figure 34 for $n = 8$.

Andreev's theorem provides the existence of a compact right-angled polyhedron R_n realizing this abstract polyhedron because it contains no prismatic 3-circuits or prismatic 4-circuits. (In fact, the work of Löbell predates that of Andreev by many years, and one can also verify the existence of R_n as an appropriate truncation and gluing of compact tetrahedra.) We refer to the group generated by reflections in the faces of R_n by Γ_n and the corresponding orbifold by $O_{\text{Löbell}}(n) = \mathbb{H}^3/\Gamma_n$.

Note 3.2. While we restrict our attention to the orbifold $O_{\text{Löbell}}(n)$ in this paper, we mention that the first example of a closed hyperbolic manifold was constructed by Löbell [Löbell 31] in 1931 by an appropriate gluing of eight copies of R_5. Generalizing this notion, Vesnin [Vesnin 87] has described a convenient algebraic method to construct a torsion-free subgroup $\Gamma'_n \subset \Gamma_n$ of index 8. This, the *nth Löbell manifold*, is the compact, orientable hyperbolic manifold $M_{\text{Löbell}}(n) := \mathbb{H}^3/\Gamma'_n$. Naturally, $M_{\text{Löbell}}(n)$ is an eightfold (orbifold) cover of $O_{\text{Löbell}}(n)$. We refer the reader to the nice exposition in [Vesnin 87, Mednykh and Vesnin 03] for the details. The delightful paper [Reni 97] provides further details on the construction of hyperbolic manifolds and orbifolds and finite covers of right-angled polyhedra.

Table 2 contains data computed using SnapPea for the $n = 5, \ldots, 8$ Löbell orbifolds.

The column labeled "computed volume" gives the volume as computed in SnapPea, whereas "theoretical volume" provides the volume of $O_{\text{Löbell}}(n)$ using explicit formulas from [Vesnin 98]. (In fact, we have divided the volume formula presented in [Vesnin 98] by 8, because those authors study the volume of the eightfold cover $M_{\text{Löbell}}(n)$.) If we let

$$\theta = \frac{\pi}{2} - \arccos\left(\frac{1}{2\cos(\pi/n)}\right),$$

then

$$\begin{aligned}\mathrm{Vol}(O_{\text{Löbell}}(n)) = \frac{n}{2}\Big(2\Lambda(\theta) + \Lambda\left(\theta + \frac{\pi}{n}\right) + \Lambda\left(\theta - \frac{\pi}{n}\right) \\ - \Lambda\left(2\theta + \frac{\pi}{2}\right)\Big),\end{aligned} \tag{3–2}$$

where Λ is the Lobachevsky function.

Notice that for each of the Löbell orbifolds that we computed, the volume computed in SnapPea agrees perfectly (within the six digits of precision available) with that given by (3–2).

3.3 An Orbifold Due to Mednykh and Vesnin

In a way similar to the construction of Löbell manifolds, Mednykh and Vesnin describe in [Mednykh and Vesnin 03] a compact three-dimensional hyperbolic manifold G that forms a twofold branched cover over the geometric

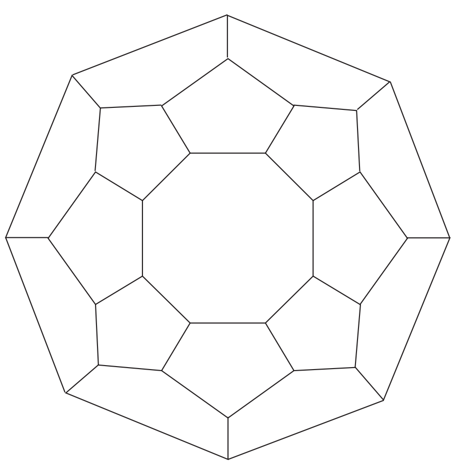

FIGURE 34. The Löbell polyhedron for $n = 8$.

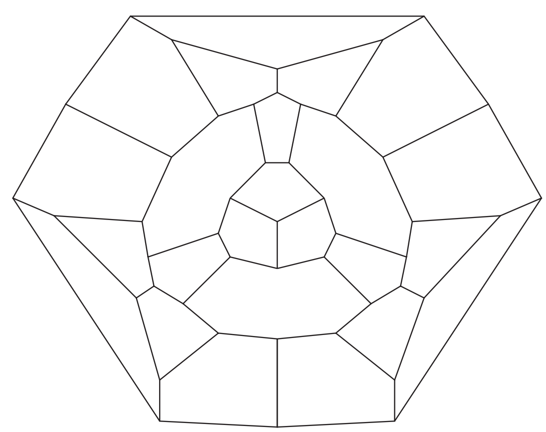

FIGURE 35. Combinatorial description of an orbifold due to Mednykh and Vesnin.

$O_{\text{Löbell}}(5)$ (Dodecahedron)	Computed Volume: 4.306208	Theoretical Volume: 4.3062076007
Short Geodesics	60 mI 2.122550	60 mI $2.122550 + i \cdot \pi$
	60 mI 2.938703	60 mI $2.938703 + i \cdot \pi$
	126 mI 3.233843	60 mI 3.579641
	60 mI $3.783112 + i \cdot 1.376928$	12 3.835986
	12 $3.835986 + i \cdot \pi$	60 mI $3.835986 + i \cdot \pi$
	60 mI 3.966774	60 mI $4.0270318 + i \cdot 2.264758$
$O_{\text{Löbell}}(6)$	Computed Volume: 6.023046	Theoretical Volume: 6.0230460200
Short Geodesics	36 mI 1.762747	12 mI $1.762747 + i \cdot \pi$
	37 mI 2.292431	12 mI $2.292431 + i \cdot \pi$
	48 mI 2.633916	24 mI $2.633916 + i \cdot \pi$
	36 mI 2.887271	24 mI $2.887271 + i \cdot \pi$
	48 mI 3.088970	12 mI $3.154720 + i \cdot 1.312496$
	24 mI 3.256614	36 mI $3.256614 + i \cdot \pi$
$O_{\text{Löbell}}(7)$	Computed Volume: 7.563249	Theoretical Volume: 7.5632490914
Short Geodesics	42 mI 1.611051	14 mI $1.611051 + i \cdot \pi$
	1 mI 1.823106	42 mI 2.388409
	14 mI $2.388409 + i \cdot \pi$	14 mI 2.512394
	14 mI $2.512394 + i \cdot \pi$	14 mI 2.601666
	70 mI 2.898149	14 mI $2.898149 + i \cdot 1.280529$
	42 mI $2.898149 + i \cdot \pi$	14 mi $3.031090 + i \cdot \pi$
$O_{\text{Löbell}}(8)$	Computed Volume: 9.019053	Theoretical Volume: 9.0190527274
Short Geodesics	49 mI 1.528571	16 mI $1.528571 + i \cdot \pi$
	80 mI 2.448452	32 mI $2.448452 + i \cdot \pi$
	16 mI $2.760884 + i \cdot 1.261789$	32 mI 2.914035
	48 mI $2.914035 + i \cdot \pi$	160 mI 3.057142
	32 mI $3.057142 + i \cdot \pi$	16 mI $3.461816 + i \cdot 2.650944$
	64 mI 3.553688	32 mI $3.553688 + i \cdot \pi$

TABLE 2. Volumes and length spectra for Löbell orbifolds.

O_{MV}	Computed Volume: 6.023046	Theoretical Volume: unknown
Short Geodesics	9 mI 0.989308	3 mI $0.989308 + i \cdot \pi$
	9 mI 1.183451	3 mI $1.183451 + i \cdot \pi$
	18 mI 1.834468	6 mI $1.834468 + i \cdot \pi$
	18 mI 1.859890	6 mI $1.859890 + i \cdot \pi$
	27 mI 1.882318	9 mI $1.882318 + i \cdot \pi$
	6 mI 1.978616	3 mI $1.978616 + i \cdot \pi$
	9 mI 2.214787	3 mI $2.214787 + i \cdot \pi$
	18 mI 2.252719	6 mI $2.252719 + i \cdot \pi$
	6 mI 2.366902	3 mI $2.366902 + i \cdot \pi$
	6 mI 2.433170	6 mI $2.433170 + i \cdot \pi$
	6 mI 2.446977	6 mI $2.446977 + i \cdot \pi$

TABLE 3. Computed volume and length spectra for the Mednykh and Vesnin Orbifold.

3-sphere $\mathbb{S}^3$. They call manifolds with such a covering property over $\mathbb{S}^3$ "hyperelliptic," generalizing the classical notion of hyperelliptic Riemann surfaces. See also [Mednykh 90, Mednykh et al. 02, Mednykh and Reni 01].

The combinatorial polyhedron considered by Mednykh and Vesnin (and apparently originally due to Grinbergs) is depicted in Figure 35.

This abstract polyhedron has no prismatic 3-circuits or prismatic 4-circuits, so Andreev's theorem guarantees the existence of a polyhedron R_{MV} realizing it with $\pi/2$ dihedral angles. We denote the group generated by reflections in the faces of R_{MV} by Γ_{MV} and the orbifold by O_{MV}. Combinatorial details on the construction of M_{MV} as a 16-fold cover of O_{MV} can be found in [Mednykh and Vesnin 03].

Table 3 contains invariants of the orbifold $O_{\text{MV}} = \mathbb{H}^3/\Gamma_{\text{MV}}$ obtained by entering an explicit list of generators for Γ_{MV} into SnapPea.

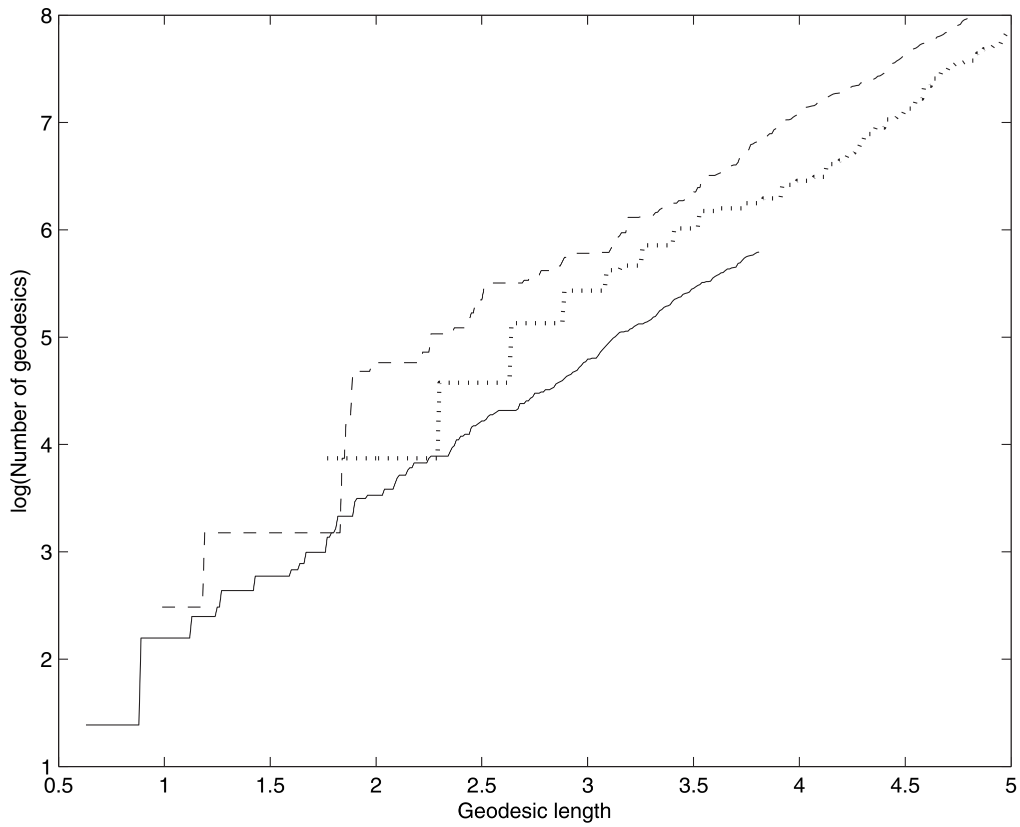

FIGURE 36. Spectral Staircases for the $O_{\text{Lambert}}(3,4,5)$ (solid line), $O_{\text{Löbell}}(6)$ (dotted line), and O_{MV} (dashed line).

As an application, we obtain the estimate

$$\text{Vol}(M_{\text{MV}}) = 16 \cdot 15.608119 = 249.729904$$

using that M_{MV} is a 16-fold orbifold cover over O_{MV}.

3.4 Spectral Staircases

For a given hyperbolic manifold or orbifold M, the "spectral staircase" is a plot of the number of closed geodesics of length less than l, which we denote by $N(l)$, as a function of l. (In fact, it is much more common to plot $\log(N(l))$ due to the exponential growth predicted by (3–3) below.) The spectral staircase provides both a nice way to graphically display the spectrum of M and an illustration of the classical result in [Margulis 69], where the following universal formula for the asymptotics of $N(l)$ is proved:

$$N(l) \sim \frac{\exp(\tau l)}{\tau l} \quad \text{as } l \to \infty, \tag{3–3}$$

where the constant τ is the topological entropy, which for hyperbolic space $\mathbb{H}^d$ is given by $\tau = d - 1$. For an exposition and nice experimental work on spectral staircases, see [Inoue 01] and the references therein.

We compute these spectral staircases for $O_{\text{Lambert}}(3,4,5)$, $O_{\text{Löbell}}(6)$, and O_{MV}, displaying the results in Figure 36. (The data for $O_{\text{Lambert}}(3,4,5)$ end at roughly $l = 3.8$. SnapPea encounters an error computing at this length, probably due to the comparatively small dihedral angles of $O_{\text{Lambert}}(3,4,5)$.)

4. QUESTIONS FOR FURTHER STUDY

We present a noncomprehensive list of interesting questions for further study:

- Determine whether there is a faster way of computing Andreev polyhedra (possibly using CirclePack or Orb).

- Construct manifold covers of the polyhedral orbifolds that were considered in Section 3, including the Löbell manifolds [Vesnin 87], the "small covers of the dodecahedron" [Garrison and Scott 03], and the hyperelliptic manifold [Mednykh and Vesnin 03]. Such a construction could potentially lead to computations of many additional interesting invariants of these manifolds using SnapPea, as well as computations of drilling and Dehn fillings on them (which would also be possible in SnapPea).

- Related question: use the program Snap to compute arithmetic invariants for these manifolds.
- Related question: using Snap, or the ideas used in Snap [Coulson et al. 00], study the arithmetic invariants of polyhedral reflection groups.[8]
- Perform a study of volumes of hyperbolic polyhedra corresponding to general angles in A_C. (While SnapPea computes volumes only for polyhedra with discrete reflection groups, the functions from the SnapPea kernel could probably be used for this more general study.)

5. CONSTRUCTING COMPACT POLYHEDRA AND THEIR REFLECTION GROUPS

The computer program described in this paper is a functional but slightly rough collection of Matlab (or Octave) scripts. Using a single command, the program produces a polyhedron realizing a simple abstract polyhedron C with all dihedral angles $\frac{2\pi}{5}$. However, one must do a little bit more work to construct a polyhedron realizing $(C, \mathbf{a})$ of truncated or compound type. These additional steps are not automatic in the program, but one can follow the description in this paper step by step to do them "by hand." Please see the README file enclosed with the program for further information.

There are two ways to output a polyhedron that has been constructed using this program: the *Object File Format* (e.g., `filename.off`) and the *Generators File Format* (e.g., `filename.txt`). The *Object File Format* output can be read into Geomview and displayed nicely in the Poincaré ball model there. The *Generators File Format* is for SnapPea, and (if the polyhedron output this way has dihedral angles that are proper integer submultiples of π) this file can be loaded into SnapPea.

An analysis of the computational complexity of this method would be quite involved and is not feasible at this point. In fact, the computational complexity of Newton's method is quite difficult [Shub and Smale 93a, Shub and Smale 93b, Shub and Smale 93c, Shub and Smale 96, Álvarez 06].

In practice, on a contemporary PC running Linux, the most complicated construction in this paper took approximately two minutes; it is by no means fast, but certainly usable. We expect that this program can be used to construct all polyhedra having no more than thirty faces and having dihedral angles bounded away from ∂A_C (with the exception of the part of ∂A_C corresponding to dihedral angles $\pi/2$, where there should be no problem). The number of iteration steps in each homotopy (the parameter K from Section 2.4) and the parameter ϵ used in the Whitehead move (see Section 2.5) may well need to be modified in special circumstances. With improvements of the program, perhaps by implementing it in a faster programming language, and, if necessary, in a higher-precision arithmetic, we expect the same to be possible for up to one hundred faces, or possibly more.

[8] This has recently been carried out as described in [Antolín-Camarena et al. 07].

ACKNOWLEDGMENTS

The author gratefully thanks John H. Hubbard for suggesting that he write the computer program and for providing an outline for using the homotopy method in combination with Andreev's proof. It was this suggestion that led to the discovery of the error in Andreev's proof [Roeder et al. 07, Roeder 04] and eventually to a working program. The author has greatly benefited from many discussions with William D. Dunbar, and he also thanks Rodrigo Perez and Travis Waddington for providing suggestions about the manuscript and attached computer files.

The computer program SnapPea, written by Jeff Weeks and his collaborators, has allowed for the exciting applications in Section 3 of this paper. The author thanks Jeff Weeks and his collaborators for writing this wonderful program, and also thanks Jeff Weeks for helpful personal communications.

The author also gratefully thanks the referee who offered many suggestions that have led to a clearer explanation of why we use the technique that we use. His or her comments have also provided the inspiration for the last two sections of this paper, and significant further research in these directions.

The author was partially supported by a U.S. National Defense Science and Engineering Fellowship and by the Fields Institute as a Jerrold E. Marsden postdoctoral fellow.

REFERENCES

[Adams et al. 91] Colin Adams, Martin Hildebrand, and Jeffrey Weeks. "Hyperbolic Invariants of Knots and Links." *Trans. Amer. Math. Soc.* 326:1 (1991), 1–56.

[Alekseevskij et al. 93] D. V. Alekseevskij, È. B. Vinberg, and A. S. Solodovnikov. "Geometry of Spaces of Constant Curvature." In *Geometry, II*, pp. 1–138, Encyclopaedia Math. Sci. 29. Berlin: Springer, 1993.

[Allgower and Georg 90] Eugene L. Allgower and Kurt Georg. *Numerical Continuation Methods: An Introduction.* New York: Springer-Verlag, 1990.

[Álvarez 06] Carlos Beltrán Álvarez. "Sobre el Problema 17 de Smale: Teoría de la intersección y geometría integral." PhD thesis, Universidad de Cantabria, 2006.

[Andreev 70a] E. M. Andreev. "On Convex Polyhedra in Lobačevskii Spaces (English Translation). *Math. USSR Sbornik* 10 (1970), 413–440.

[Andreev 70b] E. M. Andreev. "On Convex Polyhedra in Lobachevsky Spaces" (in Russian). *Mat. Sb.* 81:123 (1970), 445–478.

[Antolín-Camarena et al. 07] Omar Antolín-Camarena, Gregory R. Maloney, and Roland K. W. Roeder. "Computing Arithmetic Invariants for Hyperbolic Reflection Groups." Preprint, arXiv:0708.2109, 2007.

[Bao and Bonahon 02] Xiliang Bao and Francis Bonahon. "Hyperideal Polyhedra in Hyperbolic 3-Space." *Bull. Soc. Math. France*, 130:3 (2002), 457–491.

[Blum et al. 98] Lenore Blum, Felipe Cucker, Michael Shub, and Steve Smale. *Complexity and Real Computation*. New York: Springer-Verlag, 1998.

[Bowers and Stephenson 96] Phil Bowers and Kenneth Stephenson. "A Branched Andreev–Thurston Theorem for Circle Packings of the Sphere." *Proc. London Math. Soc. (3)* 73:1 (1996), 185–215.

[Chow and Luo 03] Bennett Chow and Feng Luo. "Combinatorial Ricci Flows on Surfaces." *J. Differential Geom.* 63:1 (2003), 97–129.

[Coulson et al. 00] David Coulson, Oliver A. Goodman, Craig D. Hodgson, and Walter D. Neumann. "Computing Arithmetic Invariants of 3-Manifolds." *Experiment. Math.* 9:1 (2000), 127–152.

[Díaz 97] Raquel Díaz. "Nonconvexity of the Space of Dihedral Angles of Hyperbolic Polyhedra." *C. R. Acad. Sci. Paris Sér. I Math.* 325:9 (1997), 993–998.

[Díaz 06] Raquel Díaz. "A Generalization of Andreev's Theorem." *J. Math. Soc. Japan* 58:2 (2006), 333–349.

[Garrison and Scott 03] Anne Garrison and Richard Scott. "Small Covers of the Dodecahedron and the 120-Cell." *Proc. Amer. Math. Soc.* 131:3 (2003), 963–971.

[Guéritaud 04] François Guéritaud. "On an Elementary Proof of Rivin's Characterization of Convex Ideal Hyperbolic Polyhedra by Their Dihedral Angles." *Geom. Dedicata* 108 (2004), 111–124.

[Heard 05] Damian Heard. "Computation of Hyperbolic Structures on 3-Dimensional Orbifolds." PhD thesis, University of Melbourne, 2005.

[Hodgson 92] C. D. Hodgson. "Deduction of Andreev's Theorem from Rivin's Characterization of Convex Hyperbolic Polyhedra." In *Topology 90*, pp. 185–193. Berlin: De Gruyter, 1992.

[Hodgson and Weeks 94] Craig D. Hodgson and Jeffrey R. Weeks. "Symmetries, Isometries and Length Spectra of Closed Hyperbolic Three-Manifolds." *Experiment. Math.* 3:4 (1994), 261–274.

[Hubbard and Hubbard 99] John Hamal Hubbard and Barbara Burke Hubbard. *Vector Calculus, Linear Algebra, and Differential Forms*. Upper Saddle River, NJ: Prentice Hall, 1999.

[Hubbard and Papadopol 07] John H. Hubbard and Peter Papadopol. "Newton's Method Applied to Two Quadratic Equations in $\mathbb{C}^2$ Viewed as a Global Dynamical System." To appear in *Memoirs of the AMS*, 2007.

[Inoue 01] Kaiki Taro Inoue. "Numerical Study of Length Spectra and Low-Lying Eigenvalue Spectra of Compact Hyperbolic 3-Manifolds." *Classical Quantum Gravity* 18:4 (2001), 629–652.

[Inoue 07] Taiyo Inoue. "Organizing Volumes of Right Angled Hyperbolic Polyhedra." PhD thesis, University of California, Berkeley, 2007.

[Kantorovič 49] L. V. Kantorovič. "On Newton's Method." *Trudy Mat. Inst. Steklov.* 28 (1949), 104–144.

[Kellerhals 89] Ruth Kellerhals. "On the Volume of Hyperbolic Polyhedra." *Math. Ann.* 285:4 (1989), 541–569.

[Löbell 31] F. Löbell. "Beispiele geschlossener dreidimensionaler Clifford-Kleinische Räume negativer Krümmung." *Ber. Sächs. Akad. Wiss.* 83 (1931), 168–174.

[Marden and Rodin 90] A. Marden and B. Rodin. "On Thurston's Formulation and Proof of Andreev's Theorem." In *Computational Methods and Function Theory*, pp. 103–115, Lecture Notes in Mathematics 1435. New York: Springer-Verlag, 1990.

[Margulis 69] G. A. Margulis. "Certain Applications of Ergodic Theory to the Investigation of Manifolds of Negative Curvature." *Functional Anal. Appl.* 3:4 (1969), 335–336.

[Mednykh 90] A. D. Mednykh. "Three-Dimensional Hyperelliptic Manifolds." *Ann. Global Anal. Geom.* 8:1 (1990), 13–19.

[Mednykh and Reni 01] Alexander Mednykh and Marco Reni. "Twofold Unbranched Coverings of Genus Two 3-Manifolds Are Hyperelliptic." *Israel J. Math.* 123 (2001), 149–155.

[Mednykh and Vesnin 03] Alexander Mednykh and Andrei Vesnin. "Colourings of Polyhedra and Hyperelliptic 3-Manifolds." In *Recent Advances in Group Theory and Low-Dimensional Topology (Pusan, 2000)*, pp. 123–131, Res. Exp. Math. 27, Berlin: Heldermann, Lemgo, 2003.

[Mednykh et al. 02] Alexander Mednykh, Marco Reni, Andrei Vesnin, and Bruno Zimmermann. "Three-Fold Coverings and Hyperelliptic Manifolds: A Three-Dimensional Version of a Result of Accola." *Rend. Istit. Mat. Univ. Trieste* 32 (suppl. 1) (2002), 181–191.

[Poincaré 83] Henri Poincaré. "Mémoire sur les groupes kleinéens." *Acta Math.* 3 (1883), 49–92.

[Reni 97] Marco Reni. "Dihedral Branched Coverings of Hyperbolic Orbifolds." *Geom. Dedicata* 67:3 (1997), 271–283.

[Rivin 93] Igor Rivin. "On Geometry of Convex Ideal Polyhedra in Hyperbolic 3-Space." *Topology* 32:1 (1993), 87–92.

[Rivin 96] Igor Rivin. "A Characterization of Ideal Polyhedra in Hyperbolic 3-Space." *Ann. of Math. (2)* 143:1 (1996), 51–70.

[Rivin and Hodgson 93] I. Rivin and C. D. Hodgson. "A Characterization of Compact Convex Polyhedra in Hyperbolic 3-Space." *Invent. Math.* 111 (1993), 77–111.

[Roeder 04] Roland K. W. Roeder. "Le théorème d'Andreev sur polyèdres hyperboliques." PhD thesis (in English), Université de Provence, Aix-Marseille 1, 2004.

[Roeder 06] Roland K. W. Roeder. "Compact Hyperbolic Tetrahedra with Nonobtuse Dihedral Angles." *Publicacions Matemàtiques* 50:1 (2006), 211–227.

[Roeder 07] Roland K. W. Roeder. "A Degenerate Newton's Map in Two Complex Variables: Linking with Currents." *J. Geometric Analysis* 17:1 (2007), 107–146.

[Roeder et al. 07] Roland K. W. Roeder, John H. Hubbard, and William D. Dunbar. "Andreev's Theorem on Hyperbolic Polyhedra." *Les Annales de l'Institute Fourier* 57:3 (2007), 825–882.

[Schlenker 98] Jean-Marc Schlenker. "Métriques sur les polyèdres hyperboliques convexes." *J. Differential Geom.* 48:2 (1998), 323–405.

[Schlenker 00] J.-M. Schlenker. "Dihedral Angles of Convex Polyhedra." *Discrete Comput. Geom.* 23:3 (2000), 409–417.

[Schlenker 06] Jean-Marc Schlenker. "Hyperbolic Manifolds with Convex Boundary." *Invent. Math.* 163:1 (2006), 109–169.

[Shub and Smale 93a] Michael Shub and Steve Smale. "Complexity of Bézout's Theorem. I. Geometric Aspects." *J. Amer. Math. Soc.* 6:2 (1993), 459–501.

[Shub and Smale 93b] M. Shub and S. Smale. "Complexity of Bézout's Theorem. II. Volumes and Probabilities." In *Computational Algebraic Geometry (Nice, 1992)*, pp. 267–285, Progr. Math. 109. Cambridge: Birkhäuser, 1993.

[Shub and Smale 93c] Michael Shub and Steve Smale. "Complexity of Bézout's Theorem. III. Condition Number and Packing." *J. Complexity* 9:1 (1993), 4–14.

[Shub and Smale 96] Michael Shub and Steve Smale. "Complexity of Bézout's Theorem. IV. Probability of Success; Extensions." *SIAM J. Numer. Anal.* 33:1 (1996), 128–148.

[Thurston 80] W. P. Thurston. *The Geometry and Topology of 3-Manifolds*. Princeton: Princeton University Press, 1980.

[Vesnin 87] Andrei Vesnin. "Three-Dimensional Hyperbolic Manifolds of Löbell Type." *Siberian Math. J.* 28:5 (1987), 731–733.

[Vesnin 98] Andrei Vesnin. "Volumes of Löbell 3-Manifolds." *Math. Notes* 64:1-2 (1998), 15–19.

[Vinberg 67] È. B. Vinberg. "Discrete Groups Generated by Reflections in Lobačevskiĭ Spaces." *Mat. Sb. (N.S.)* 72:114, 471–488; correction, ibid. 73:115 (1967), 303.

[Vinberg 85] È. B. Vinberg. "Hyperbolic Groups of Reflections." *Russian Math. Surveys* 40:1 (1985), 31–75.

[Vinberg 91] È. B. Vinberg. "The Volume of Polyhedra on a Sphere and in Lobachevsky Space." In *Algebra and Analysis (Kemerovo, 1988)*, pp. 15–27, Amer. Math. Soc. Transl. Ser. 2, 148. Providence: Amer. Math. Soc., 1991.

[Vinberg and Shvartsman 93] È. B. Vinberg and O. V. Shvartsman. "Discrete Groups of Motions of Spaces of Constant Curvature." In *Geometry, II*, pp. 139–248, Encyclopaedia Math. Sci. 29 Berlin: Springer-Verlag, 1993.

Roland K. W. Roeder, Department of Mathematics, University of Toronto, Toronto, Ontario, Canada M5S 2E4 (rroeder@math.utoronto.ca)

Received March 26, 2006; accepted in revised form October 31, 2006.